Biodegradable magnesium alloys for orthopaedic applications

Yu Lu[1], Subodh Deshmukh[2], Ian Jones[1], Yu-Lung Chiu[1,]*

Key Words:
biodegradability; magnesium alloys; mechanical behaviour; microstructure; orthopaedic application

From the Contents

ABSTRACT

There is increasing interest in the development of bone repair materials for biomedical applications. Magnesium (Mg)-based alloys have a natural ability to biodegrade because they corrode in aqueous media; they are thus promising materials for orthopaedic device applications in that the need for a secondary surgical operation to remove the implant can be eliminated. Notably, Mg has superior biocompatibility because Mg is found in the human body in abundance. Moreover, Mg alloys have a low elastic modulus, close to that of natural bone, which limits stress shielding. However, there are still some challenges for Mg-based fracture fixation. The degradation of Mg alloys in biological fluids can be too rapid, resulting in a loss of mechanical integrity before complete healing of the bone fracture. In order to achieve an appropriate combination of bio-corrosion and mechanical performance, the microstructure needs to be tailored properly by appropriate alloy design, as well as the use of strengthening processes and manufacturing techniques. This review covers the evolution, current strategies and future perspectives of Mg-based orthopaedic implants.

***Corresponding author:**
Yu-Lung Chiu,
y.chiu@bham.ac.uk.

http://doi.org/10.12336/biomatertransl.2021.03.005

How to cite this article:
Lu, Y.; Deshmukh, S.; Jones, I.; Chiu, Y. Biodegradable magnesium alloys for orthopaedic applications. *Biomater Transl.* **2021**, *2*(3), 214-235.

Introduction

A biomaterial is defined as a material intended to interface with biological systems to evaluate, treat, augment or replace any tissue, organ or function of the body.[1, 2] Commonly, pacemakers, stents, sutures, bone plates and screws, needles, knee joints and catheters all constitute biomaterials. Biomaterials are used across a wide range of applications and have become a major industry in the 21st century. The traditional metallic biomaterial requires that metals are as inert as possible in order to minimise the immune response and reduce the corrosion of the material itself in the physiological environment of the body. Typically, these biomaterials are stainless steels, titanium (Ti) alloys and cobalt–chrome-based alloys. After decades of developing improved corrosion-resistant metallic biomaterials, the design and application of biodegradable metals are currently under the spotlight. A biodegradable material is expected to degrade gradually *in vivo*, with an appropriate host response elicited by released corrosion products, and then to dissolve completely upon fulfilling the mission of assisting with tissue healing while leaving no implant residues.[3] The materials should be non-toxic or made up of metallic elements which can be metabolised by the human body. Therefore, magnesium (Mg)-based biodegradable alloys are a promising material for clinical applications.

Extensive research so far suggests a bright future for biodegradable Mg-based orthopaedic implants. However, new fabrication approaches, updated design strategies and enhanced clinical requirements are emerging. Thus, up-to-date progress and development of biodegradable Mg alloys over recent decades are presented in this review paper by searching google scholar. Firstly, we summarise orthopaedic applications and principles, traditional implant components (especially Ti), potential use of Mg in real clinical applications, degradation mechanisms and role of Mg in the human body. Monolithic Mg alloy components are comprehensively discussed focusing on the effects of alloying elements, microstructural evolution (grain size, second phases, twins, texture, dislocations etc.),

mechanical and bio-corrosion performance testing, *in vitro* and *in vivo* evaluation and biocompatibility assessment. Moreover, recent novel structural developments are indicated, including Mg-based bulk metallic glasses (BMGs), Mg metal matrix composites (MMCs) and porous structure. The fabrication methods, mechanical properties, biodegradation performance, and *in vitro* and *in vivo* behaviours of these Mg materials are introduced. Finally, this review discusses the future perspectives and challenges for designing the next generation of biodegradable Mg-based alloys for orthopaedic applications. The smart tailoring of alloys, novel manufacturing techniques and relatively innovative three-dimensional model design, mathematical modelling and effective transformation from designed Mg materials to safe clinical applications are emphatically proposed for future developments.

Design of orthopaedic implants

Bone is a hard biological tissue formed of cells embedded in a matrix, which consists of an organic (90% collagen and 10% amorphous) ground substance reinforced by a mineral phase. Calcium phosphate ($Ca_3(PO_4)_2$) and calcium carbonate ($CaCO_3$) are the main constituents of bone mineral. Bone serves as a protector for organs and provides mechanical stability to the body, making movement possible. There are two types of bone, cortical (compact or Haversian) and cancellous (spongy or trabecular) bone.[4, 5]

Bone remodelling is a continuous process of bone resorption and formation, to provide maximum strength with minimum mass. Bone has a strong capability to regain its lost strength through the healing process. However, the internal fixation of broken bones only became possible via aseptic techniques for open fracture reduction and direct fixation with metallic hardware.[6] Thus, supportive orthopaedic implants are necessary to fix the bone when a fracture occurs. Orthopaedic implants are medical devices which can be used to replace or provide fixation of bone, or replace the articulating surfaces of a joint. Typically, orthopaedic implants include plates, nails and screws. Fracture fixation is used to reduce interfragmentary movement.

There are several types of plates: compression plates, buttress plates, neutralisation plates and bridging plates. Compression plates are used to bring the two fracture ends of the bones close to each other and provide sufficient stability using dynamic pressure between the fragments, which promotes bone healing. Buttress plates are especially used around joints (such as knees and ankles) to hold together fractures at the ends of long bones; preventing axial forces from distorting the initial reduction.[7] These plates can be moved with the body because they are contoured. Neutralisation plates are a category of plate which bridges the fracture and protects the screws or other devices from bending and torsional loading.[8] Bridging plates are designed to provide stability when multi-fragmentary long bone fractures occur; they can offer the correct length and alignment and promote secondary bone healing.[8] This is because they preserve the blood supply to the fragments without disrupting the damaged area.

The principle of meticulous anatomical reduction of each fracture fragment by direct fracture exposure and subsequent fixation by compression plating, as practised by surgeons through the 1980s,[9] required extensive soft tissue intervention. The application of locking plates coincided with the development of minimally-invasive fracture fixation, which has resulted in important changes in fracture management.[6, 10] The most common treatment options for the fixation of fractures are locking compression plates and interlocking nails, as shown in **Figure 1**.[11, 12]

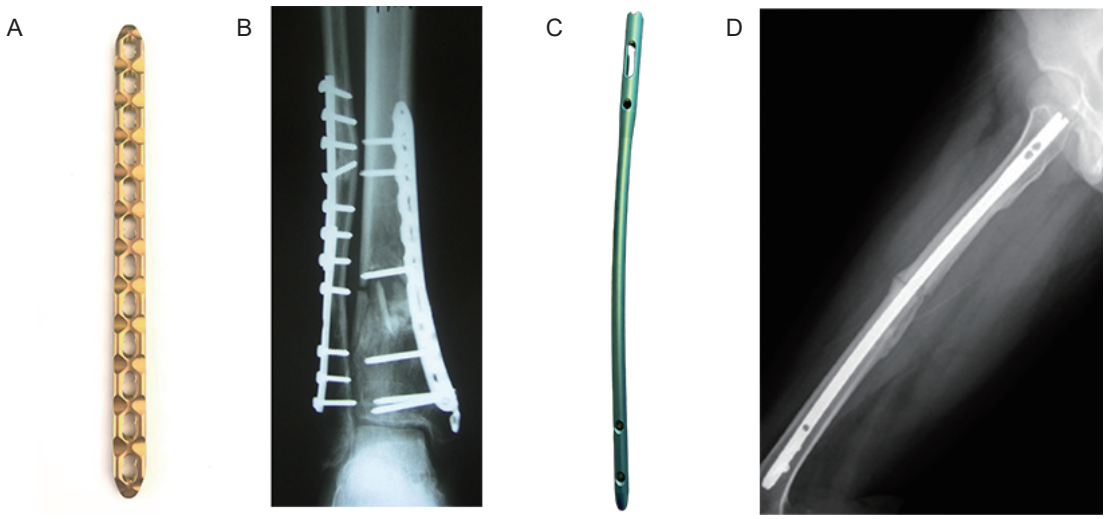

Figure 1. (A) Locking compression plate. (B) Radiograph of distal tibial fracture treated with a locking plate. Reprinted from Bastias et al.[11] Copyright 2014 European Foot and Ankle Society. (C) Interlocking nail. (D) Radiograph of femoral fracture treated with locking nail. Reprinted from Hsu et al.[12] Copyright 2019, with permission from Elsevier.

1 School of Metallurgy and Materials, University of Birmingham, Birmingham, UK; 2 Sandwell and West Birmingham Hospitals NHS Trust, Birmingham, UK

The principles of locking compression plates, nails and screws are illustrated in **Figure 2**.[8] A locking plate provides fixation with absolute stability for two-part fracture patterns, where the bone fragments can be compressed.[13] Furthermore, the addition of an orthopaedic screw across the fracture and through the plate enhances the stability. Orthopaedic screws are used to tighten up damaged areas, which are one of the tenets of orthopaedic fixation. They reduce the gap between the bones. Lag screws are used to achieve interfragmentary compression, which protects the fractured bone from bending, being rotated and from trivial loading forces. The interlocking nail is basically an intramedullary pin, providing absolute stability to maintain alignment and position, including the prevention of rotation.[14] The mechanical properties of an implant significantly affect the stability of fracture fixation provided by orthopaedic implants/devices.

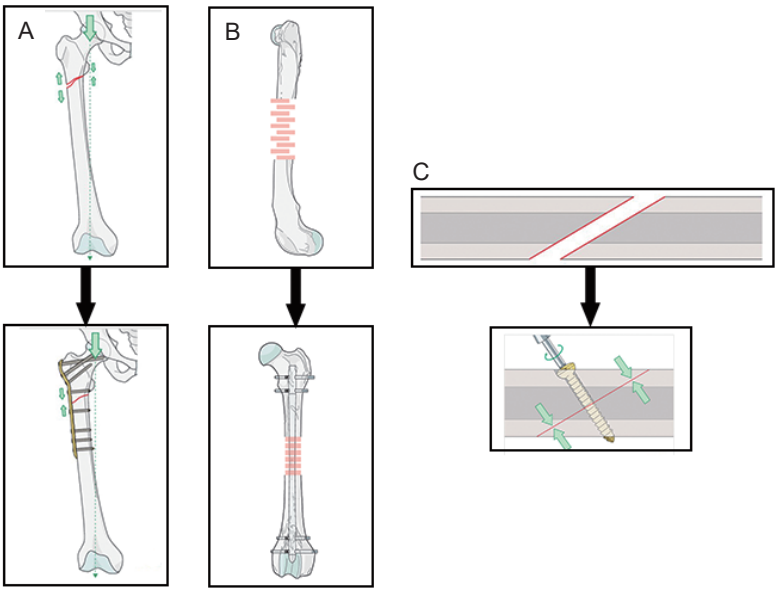

Figure 2. (A–C) Principles of locking compression plate (A), intramedullary nailing (B), and screw (C).[8]

Common metallic alloys for orthopaedic application

Ti, stainless steel and cobalt–chromium (Co-Cr) alloys have been employed as permanent implants. Stainless steel and Co-Cr alloys are the first generation of inert metallic implants. Stainless steel has been used to manufacture bone plates, screws and pins, which have excellent mechanical properties but high modulus and poor wear resistance. Co-Cr alloys have good mechanical properties and superior corrosion resistance, but high modulus and are difficult to machine. Ti alloys are 'second generation' and are used for fracture fixation and femoral hip stems. Ti alloys have excellent corrosion resistance, good biocompatibility and high mechanical strength, but poor wear resistance, poor bending ductility and come at a high cost.[15] The objective of orthopaedic implants is to produce absolute stability, abolishing all interfragmentary motion. The implant material must have adequate mechanical properties. The mechanical performance characteristics of unalloyed Ti, stainless steel and Co-Cr alloys for surgical implant applications are listed in **Table 1**.[16-18]

Table 1. Mechanical performance of commercial pure (CP) titanium, stainless steel and cobalt–chromium alloys for surgical implant application.

	Yield strength (MPa)	Ultimate tensile strength (MPa)	Elongation (%)
CP Ti			
Grade 1	170	240	24
Grade 2	275	345	20
Grade 3	380	450	18
Grade 4	483	550	15
Stainless steel			
18Cr-14Ni-2.5Mo			
Annealed	190	490	40
Cold-worked	690	860	12
Co-28Cr-6Mo			
Annealed	517	897	20
Hot-worked	700	1000	12

Note: Superscript a indicates a different grade of CP Ti which often means a different oxygen content. Data are from ASTM International.[16-18]

Bone is a living tissue which undergoes constant remodelling under imposed stress. If the load supported by the implant is too large, the bone beneath will bear a reduced load and will become less dense and weaker because the stimulation and continual remodelling which maintain bone mass are absent or reduced, leading to the so-called stress-shielding phenomenon. Although Ti alloy plates (e.g. Ti–6Al–4V, CP Ti) provide less stress-shielding than stainless steel (e.g. 316L)[19] because of their lower moduli,[20, 21] the moduli are still much higher than that of human cortical bone (around 20 GPa).[22] Thus, the stress shielding effect caused by the mismatch in the elastic modulus between human bone and Ti implants is still an issue.

To address this problem, alloys such as Co-Cr-Mo and Ti-6Al-4V have been manufactured as a scaffold to reduce the modulus mismatch with natural bone.[23] Conventionally-sintered metals, however, are often very brittle. Other fabrication techniques (such as foaming agents or molten metal) also have some drawbacks, such as contamination, impurity phases, limited control of size and shape, and distribution of porosity.[24] Noticeably, mechanical wear and corrosion are associated with a long period of implantation in the body, which results in the release of some toxic ions (Cr, Ni, Co, etc.) and triggers undesirable immune responses, consequently reducing the implant's biocompatibility.[25] Moreover, difficulty in removing locking head screws made of Ti has been reported:[26] the screws cannot be removed with a normal screw driver and purpose-built devices are required.

Possible use of magnesium in surgical applications

A more promising material for use in orthopaedic application is required and one example is biodegradable Mg alloys. Natural cortical bones have a volume density ranging from 1.0 g/cm^3 to 2.1 g/cm^3 and an elastic modulus ranging from 3.0 GPa to 20.0 GPa.[27] Mg has a very low density of 1.74–2.0 g/cm^3, which is significantly lower than that of Ti alloys (~4.5 g/cm^3) and stainless steel (~8 g/cm^3).[28] Mg alloys have a relatively low elastic modulus of 41–45 GPa, compared with other traditional biomaterials (Ti-6Al-4V alloys: 110–117 GPa; 316L stainless steel: 205–210 GPa; Co-Cr alloys: 230 GPa).[29] A comparison of Mg alloys and natural bones is shown in **Table 2**.[27, 30, 31] Mg^{2+} is the fourth most abundant cation in the human body and is an essential element for the human body (the daily intake of Mg^{2+} for a normal adult is about 300–400 mg).[32-34] It has been reported that moderate Mg^{2+} ion supplementation released directly from the prosthesis itself will bring significant benefits after implant surgery, diminishing the chance of infection.[35] A number of *in vivo* and *in vitro* experiments have shown that Mg alloys have good biocompatibility.[36-38] The chief attraction of Mg alloys as orthopaedic materials, however, is biodegradability. Mg alloys can be biodegraded in the human body, which can eliminate the need for a second round of surgery for implant removal. Some *in vivo* studies have confirmed that the degradation of Mg is harmless.[37, 39, 40]

Table 2. Summary of the physical and mechanical properties of magnesium alloys in comparison with human bone.

	Density (g/cm^3)	Elastic modulus (GPa)	Tensile strength (MPa)	Fracture toughness (MPa$^{1/2}$)	Total elongation (%)
Cortical bone	1.8–2.1	3–20	35–283	3–6	1.07–2.10
Cancellous bone	1.0–1.4	NA	1.5–38	NA	NA
Magnesium alloys	1.74–2.0	41–45	150–400	15–40	2–20

Note: Different values are due to differences in ethnicity, age, testing conditions, etc. NA: not applicable. Data are from Maehara et al.[26-28]

In order to replace permanent metallic implants for orthopaedic applications, Mg alloys need to target both mechanical requirements and an appropriate degradation rate. **Figure 3** shows a schematic of the optimal relationship between provision of mechanical support and biodegradation behaviour. Initially, it is essential that the implants are strong enough to provide sustained fixation, support the injury and carry the load to give adequate time for the damaged bone tissues to heal. The implant should gradually and slowly degrade and transfer the load to the bone over time.[41] Before the injury heals, the implant has constantly to sustain the injury and provide mechanical support until the tissue regains sufficient mechanical strength. A period of 3–4 months is generally required for new bone formation and recovery of most of the bone's original strength.[42] The different healing periods relate to the different ages of the patients.

For load-bearing applications, the implant material has to have suitable mechanical properties to withstand various biomechanical forces. The mechanical properties of interest for the implant are elastic modulus, yield strength, ultimate tensile strength and ductility. To bend fixtures to fit properly requires sufficient ductility.[43] Materials with higher elastic modulus can absorb more energy and hold their shape better, and are therefore less likely to 'cut' into the bone.[44] In addition, although fast corrosion kinetics can be generally beneficial in biodegradable alloys, there is a balance to be struck and Mg alloys can have a significant problem if the corrosion rate is too high. Current Mg alloys degrade too quickly in the human body and lose function before the tissue heals.

Magnesium biodegradation in the physiological environment

The corrosion of Mg in the aqueous environment is an electrochemical phenomenon. The electrochemical degradation mechanism of Mg in aqueous solution can be described as follows and produces Mg hydroxide ($Mg(OH)_2$) and hydrogen gas (H_2):

Anodic reaction/dissolution: $Mg \rightarrow Mg^{2+} + 2e^-$ (1)

Cathodic reaction: $2H_2O + 2e^- \rightarrow 2OH^- + H_2$ (2)

Hydrolysis: $Mg + H_2O \rightarrow MgOH^+ + H^+$ (3)

Product formation: $Mg^{2+} + 2OH^- \rightarrow Mg(OH)_2$ (4)

Obviously, the hydrolysis reaction consumes H_2O and

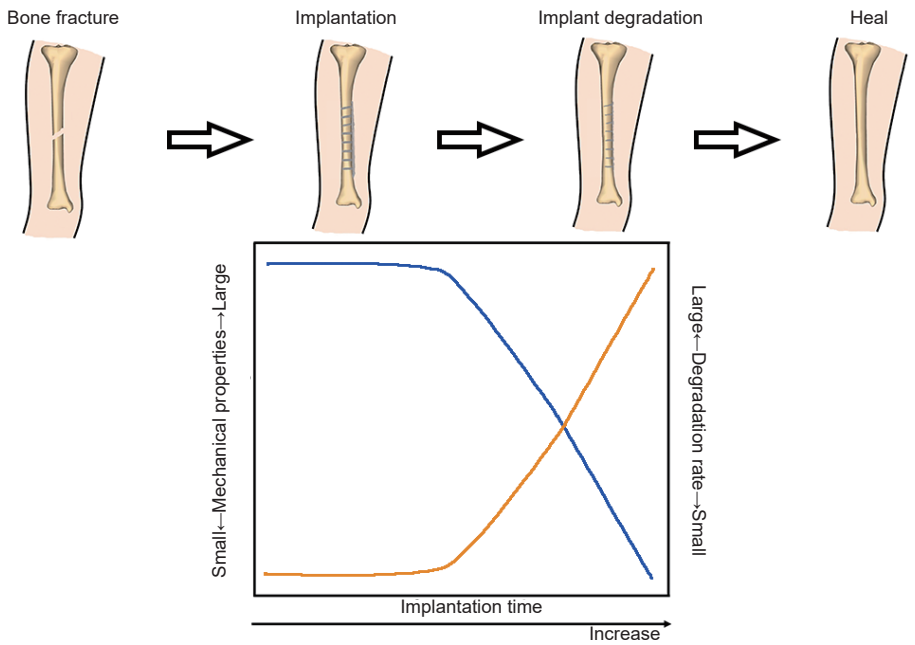

Figure 3. Optimal degradation behaviour of a magnesium-based implant in bone fracture healing. The blue and yellow lines indicate the mechanical integrity and biodegradation rate, respectively.

produces H^+, and thus reduces the pH value in the solution. The precipitation of $Mg(OH)_2$ and stabilisation of the passive film tend to occur because of pH increases due to the cathodic reaction. Alkalisation of the solution occurs over time, which is caused by the cathodic reaction and the balance between the anodic and cathodic reactions. Each Mg^{2+} formed produces two OH^- and generates one H^+. Therefore, the overall reaction results in a pH increase, which must be paid attention to when monitoring the biodegradation rate. **Figure 4** illustrates the corrosion mechanism of Mg in an aqueous environment.[45]

The processes of equations (1–4) are vividly demonstrated in **Figure 4A**. The dissolution of Mg and the formation of hydrogen and Mg hydroxide are the main features. The aggressive ion Cl^- reacts with $Mg(OH)_2$ and forms more soluble $MgCl_2$ (equation (5)).

$$Mg(OH)_2+2Cl^-\rightarrow MgCl_2+2OH^- \quad (5)$$

Further corrosion of Mg is promoted by the dissolution of $Mg(OH)_2$ due to the disappearance of the protected areas.[46] Cl^- catalyses the dissolution of Mg and directly produces $MgCl_2$, exposing the bare Mg to the solution[47, 48] (**Figure 4B**).

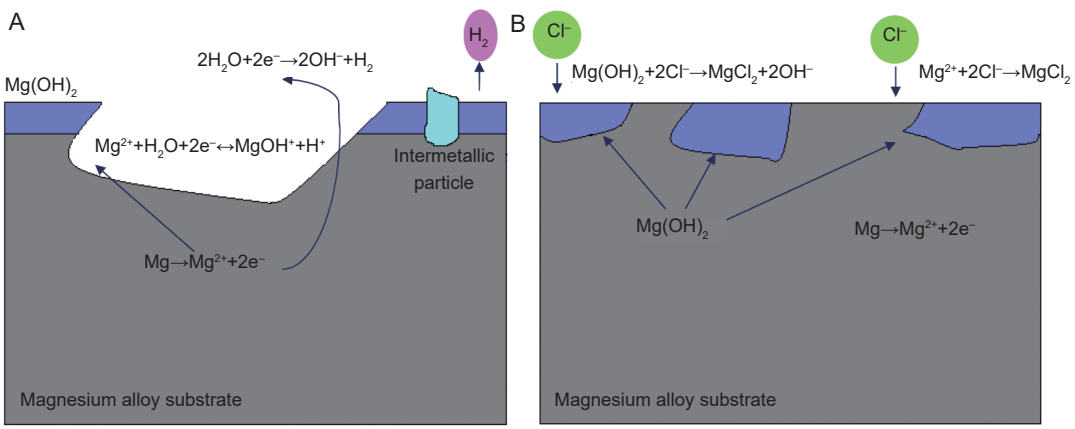

Figure 4. Schematic illustration of the corrosion of magnesium in an aqueous environment:[45] (A) The dissolution of magnesium via the anodic reaction. The cathodic reaction increases the pH and produces H_2, while hydrolysis reduces the pH. Intermetallic particles act as cathodic sites and consume the electrons produced by the anodic reaction. (B) Chloride ions in the solution attack and dissolve the $Mg(OH)_2$ film.

Following the reaction of Mg in the physiological environment, it must be mentioned that hydrogen evolves during the reaction according to the cathodic reaction. Gas cavities composed of generated hydrogen have been observed around Mg alloy implants because of insufficient diffusion.[49] The formation of these gas pockets happens during the early implantation stage (7–30 days); the gas is then gradually absorbed by the surrounding tissue.[50] It has been reported that gas formation does not have any negative effects on bone healing.[51] However, the rapid corrosion of Mg causes the quick formation of gas cavities and subcutaneous bubbles, which may reduce its mechanical strength. Thus, in order to slow hydrogen generation, the degradation rate of Mg-based alloys must be carefully controlled.

The Role of Magnesium in the Human Body

Mg is a nutrient that the body needs to stay healthy and is important for many processes. Mg is primarily found within the cells and is a cofactor in more than 300 enzymatic reactions, which are essential for the human body.[52] The presence of Mg is vital for transmission and storage of energy to be used by cells.[53] It also has a central role in cell growth and the structure and permeability of their membranes.[52, 54] It has been reported that Mg^{2+} ions are able to aid the growth of bone marrow cells through the enhancement of bone morphogenetic protein receptor recognition and Smad signalling pathways.[55] The mitogen-activated protein kinase/extracellular signal-regulated kinase pathway is one of the signalling pathways which controls the osteogenic differentiation of stem cells, and Mg^{2+} can selectively activate the mitogen-activated protein kinase/extracellular signal-regulated kinase pathway.[56] The biphasic mode of Mg^{2+} in bone repair has been recently reported by Qiao et al.[57] Mg-induced osteogenesis has been observed, suggesting the therapeutic potential of Mg^{2+} in orthopaedics.[58-60] In addition, Mg^{2+} ions affect the seeded calcium phosphate crystallisation rate and subsequent hydroxyapatite growth.[61] The total body stores of Mg are between 21 g and 28 g in the average 70 kg adult. Normal serum usually has a Mg range of 1.7 mg/dL to 2.5 mg/dL. Most of the body's Mg is in the skeletal bone mass, which accounts for more than 50% of the body's stores. The remainder is located in soft tissues, of which only 0.3% is located extracellularly. Of the total Mg consumed, approximately 30% to 50% is absorbed.[62] Too much Mg from food does not pose a health risk because the kidneys eliminate excess amounts via the urine.[63] However, a very high dose of Mg via, for example, dietary supplements or medications can result in diarrhoea that can be accompanied by nausea and abdominal cramping.[64] The daily intake allowances of Mg are summarised in **Table 3**.[65]

Table 3. Intake allowances for magnesium.

	Recommended dietary allowances for magnesium (mg)		Tolerable upper intake levels for supplemental magnesium (mg)	
Age (year)	Male	Female	Male	Female
19–30	400	310	350	350
31–50	420	320	350	350
51 or more	420	320	350	350

Note: Data are from Office of Dietary Supplements, National Institutes of Health.[65]

Application of magnesium-based alloys in orthopaedic applications

In the past, a number of investigations have been carried out on potential Mg-based implants for use in orthopaedic applications. Windhagen et al.[66] reported that compression screws made of MgYREZr alloy showed good biocompatibility and osteoconductive properties. Cortical bone screws machined from AZ31 (Mg-3Al-1Zn) alloy have been implanted into hip bone,[67] while intramedullary nails made of LAE442 (Mg-4Li-4Al-2RE) have been implanted into the marrow cavity of tibiae.[68] However, very few monolithic Mg-based components are used in load-bearing applications (such as compression plates, bridging plates etc.) because of their too-rapid biodegradation rate. Thus biodegradable Mg implants need to be further explored. Moreover, Mg-based bioceramics, bioglasses, biocomposites and 3D-printed scaffolds need to be carefully designed.

Design strategies for biodegradable magnesium alloys

Biodegradable Mg alloys require suitable mechanical and biodegradation performance in a physiological environment and, most importantly, biosafety with regard to the human body. Rather than simply applying commercial Mg alloys to the biomedical field, the alloys should also be designed with nutriology and toxicology in mind, to give a superior balanced performance. The alloying design, element selection, processing history and heat treatments significantly affect the microstructure and lead to different mechanical and corrosion behaviours.

Alloying elements

Suitable alloying elements need to be tailored to design and improve the mechanical and bio-corrosion properties of biomedical Mg alloys. **Table 4** shows a brief summary of the various alloying elements used in Mg biomaterials.[3, 38, 69-85] Alloying elements can strengthen the Mg alloys by solid solution strengthening, precipitation hardening and grain refinement strengthening. These alloying elements must have high and temperature-dependent solubility in Mg. High solubility of an alloying element can lead to significant precipitation hardening of Mg alloys, such as Mg-Al alloys, Mg-Zn alloys and Mg-rare earth (RE) alloys. Both solid solution strengthening and precipitation strengthening improve the strength, but generally cause deterioration in the ductility of Mg alloys. However, grain refinement strengthening improves both strength and ductility. It is widely acknowledged that

Table 4. The physical properties and influence of alloying elements on properties and biological impact of magnesium-based alloys.

Element	Solubility limits (wt%)	Growth restriction factor	Effects on mechanical properties	Effects on corrosion behaviour	Biological impact	Maximum daily allowable dose (mg)
Aluminium (Al)	12.7	4.32	Improves strength and ductility Grain refinement Increases castability	Decreases corrosion rate	Neurotoxic; Decreases osteoclast viability	14
Calcium (Ca)	1.34	11.94	Improves strength Grain refinement Increases castability	Decreases corrosion resistance	Most abundant mineral in the human body; Is tightly regulated by homeostasis	1400
Zinc (Zn)	6.2	5.31	Improves strength Reduces ductility at high concentration		Essential trace element (immune system, co-factor); Neurotoxic at higher concentration	15
Manganese (Mn)	2.2	0.15	Improves strength and ductility Grain refinement	Decreases corrosion rate by removing iron and other heavy metal elements into relatively harmless compounds	Essential trace element; Important role in metabolic cycle and for the immune system; Neurotoxic at higher concentration	5
Lithium (Li)	5.5		Reduces strength Improves ductility	Reduces corrosion resistance	Possible teratogenic effects	
Zirconium (Zr)	3.8	38.29	Improves strength and ductility Grain refinement			
Silicon (Si)	~0	9.25	Reduces ductility and castability	Reduces corrosion resistance	Essential mineral in human body Helps to build the immune system	
Strontium (Sr)	0.11	3.51	Improves strength and ductility; Grain refinement	Deceases corrosion rate	Trace element in human body; Stimulates bone formation	5
Yttrium (Y)	12.4	1.7	Improves strength	Same standard electrochemical potential as Mg; Decreases corrosion rate by purifying the alloy and forming a passive film	May exhibit anti-carcinogenic properties	0.016[a]
Neodymium (Nd)	3.6		Improves strength	Decreases corrosion rate by creating less noble intermetallic phase ('scavenger effect' on impurities)	May exhibit anti-carcinogenic properties	4.2[a]
Copper (Cu)			Increases strength		Causes hypotension, jaundice, etc.	

Note: Superscript a indicates that the total amount of rare earth elements (Ce, La, Nd, Pr, Y) should not exceed 4.2 mg/day. Data are from Zheng et al.[3, 38, 69-85]

the refinement efficiency of the alloying elements can be determined by their growth restriction factor.[86-88] The growth restriction factor is a measure of the segregation power of an element during solidification. It is calculated from binary phase diagrams and equals $\Sigma_i m_i C_{0,i} (k_i - 1)$, where m_i is the slope of the liquidus line (assumed to be straight), k_i is the distribution coefficient and $C_{0,i}$ is the initial concentration of element i.[89] If an element has a large growth restriction factor (such as Zr, Ca, Zn) this means that the growth-restricting effect on the solid-liquid interface of the new grains is strong, thus preventing new grains from growing into the melt.[90] These elements segregate strongly in the melt and cause intense constitutional supercooling in a diffusion layer ahead of the advancing solid/liquid interface, consequently promoting nucleation and restricting grain growth. Therefore, these elements can significantly refine the grains, which benefits both strength and ductility.

The second aspect to be considered is the effects of alloying elements on the bio-corrosion behaviour. The addition of some alloying elements can improve corrosion resistance by reacting with impurities. For example, Mn and Zn can overcome the harmful corrosion effects of impurities (such

as Fe and Ni) by transforming impurities into harmless intermetallic compounds.[91] Alloying Mg with Y can enhance the corrosion resistance, because of the formation of a stable and less chemically-reactive hydroxide protective film.[75, 92] Moreover, alloying elements which form secondary phases with a similar corrosion potential (E_{corr}) can reduce internal galvanic corrosion.

The third consideration is the biocompatibility of alloying elements. The released metallic ions resulting from the degradation of Mg alloys need to be non-toxic or to be tolerated at low concentrations, below the threshold level. Elements can be categorised into different groups: 1) nutrient elements: Ca, Zn, Si, Sr; 2) allergic elements (elements likely to cause severe hepatotoxicity or other allergic problems): Al, Co, V, Cr, Ni, Ce, La, Cu, Pr; and 3) toxic elements: Cd, Be, Pb, Ba, Th. It has been reported that some RE elements (such as Y, Nd, Ho, Dy and Gd) have little influence on cell viability and haemolysis rates, but that other RE elements (such as La, Ce, etc.) need to be carefully controlled.[93] Notably, the total amount of RE elements (Ce, La, Nd, Pr, Y) should be carefully controlled (below 4.2 mg/day).

Commercially-available Mg alloys can be divided into four major groups: 1) Al-containing Mg alloys, such as AZ31 (Mg-3Al-1Zn),[94] AZ61 (Mg-6Al-1Zn), AZ91 (Mg-9Al-1Zn) and AM60 (Mg-6Al-0.3Mn); 2) Al-free Mg alloys, such as ZK30 (Mg-3Zn-0.6Zr),[95] ZK60 (Mg-3Zn-0.6Zr) and Mg-Mn-Zn;[96] 3) RE-containing alloys, such as WE43 (Mg-4Y-3RE-0.5Zr),[94, 97] LAE442 (Mg-4Li-4Al-2RE), WZ21 (Mg-2Y-1Zn)[98] and Mg-Y;[38, 99] and 4) nutrient element-containing alloys, such as Mg-Zn,[100-102] Mg-Ca,[103] Mg-Zn-Ca,[45, 104, 105] Mg-Si[106] and Mg-Sr.[107] The large range of mechanical properties of Mg alloys is shown in **Figure 5**.[45, 84] An appropriate amount of Al, Ca and Zn can increase both the strength and ductility concurrently. Zr restricts grain growth and benefits the mechanical properties. Among these Mg-based alloys, Mg-RE-based alloys normally have a superior combined strength and elongation. Mg-Zn based-alloys are also very promising and exhibit good strength and elongation compared with other systems.

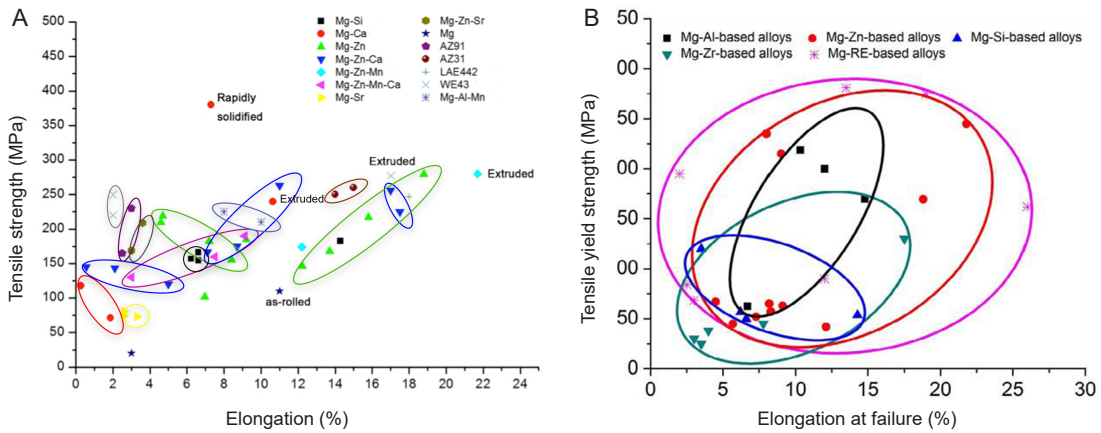

Figure 5. The tensile strength and elongation of various magnesium alloys. (A) Reprinted from Lu.[45] (B) Reprinted from Chen et al.[84] Copyright 2014, with permission from Acta Materialia Inc.

The *in vitro* and *in vivo* corrosion rates of Mg-based alloys are shown in **Table 5**.[36, 38, 39, 94, 99, 100, 103, 108-117] The *in vivo* corrosion rates of Mg-1.2Mn-1Zn,[36] Mg-0.8Ca[115] and WE43[115] alloys have been reported and compared.[118] These alloys have a low *in vivo* corrosion rate. Corrosion resistance can be modified by thermal–mechanical processing: for example, as shown in as-cast and as-extruded AZ31 alloy, as-cast and as-rolled Mg-1Zn, as-cast and as-rolled Mg-1Zr. The Mg-RE-based alloys generally show good corrosion resistance, especially after thermal–mechanical processing, for example Mg-Nd-Zn-Zr, WE43 and Mg-Gd-Zn-Zr alloys (shown in **Table 5**). Note that Witte et al. have reported that the *in vivo* (animal model) degradation of AZ91D and LAE442 alloys was very different from the *in vitro* corrosion.[109] The major reason for the differing corrosion behaviours is the dynamic nature of the *in vivo* environment and the static nature of the *in vitro* environment. In addition, the covering of proteins on implants, the remodelling of bones and possibly a protective corrosion layer in the *in vivo* environment may lead to a reduced corrosion rate.[109]

In summary, amongst these Mg-based alloys, Mg-Zn-based alloys are very promising, not only exhibiting good strength and elongation compared with other systems, but also showing enhanced corrosion resistance. Moreover, Mg-Zn alloys have good biocompatibility, because Zn is an essential trace element in the human body.

Mg-Y and Mg-Nd-based alloys normally have an excellent combination of strength and elongation, and good corrosion resistance. Regarding biosafety, the amount of Y and Nd should be controlled to be below a threshold level. It is generally accepted that the total amount of Nd and Y should not exceed 4.2 mg/day.[83, 84] Assuming that a Mg alloy implant degrades within 3 months, the total released amount of Nd and Y needs to be below 380 mg. For example, if the total weight of an implant is 6.9 g (calculated from the locking compression plate (LCP3.5-423.621)), then the total wt% of Nd and Y would need to be controlled to lie below 5wt%.

Table 5. Bio-corrosion properties of magnesium-based alloys.

Alloy	Condition	*In vitro* corrosion rate (mm/year)	*In vivo* corrosion rate (mm/year)	Reference
Mg-0.8Ca	As-extruded	–	0.5	115
Mg-1Ca	As-cast	–	1.27	103
Mg-1Al	As-cast	2.07	–	38
Mg-1Zn	As-cast	1.52	–	38
Mg-1Zn	As-rolled	0.92	–	38
Mg-1Zr	As-cast	2.2	–	38
Mg-1Zr	As-rolled	0.91	–	38
Mg-1Sn	As-cast	2.45	–	38
Mg-2Sr	As-rolled	0.37	1.01	116
Mg-3Zn	Solution treated	1.53	–	100
Mg-6Zn	As-extruded	0.07	2.32	117
Mg-8Y	As-cast	2.17	–	99
AZ31	As-cast	2	1.17	39
AZ31	As-extruded	0.21	–	94
AZ61	As-cast	0.73	–	108
AZ91D	As-cast	2.8	1.38	109
WE43	As-cast	0.26	1.56	39, 94
Mg-1.2Mn-1Zn	As-cast	–	0.45	36
Mg-1Zn-1Ca	As-cast	2.13	–	110
Mg-3Zn-0.3Ca	Solution treated	0.81	–	111
Mg-6Zn-1Ca	As-cast	9.21	–	110
Mg-4Zn-0.5Ca-0.4Mn	As-cast	0.25	–	112
Mg-3.09Nd-0.22Zn-0.44Zr	As-extruded	0.13	–	94
Mg-2Zn-1.53Y	As-extruded	0.7	–	113
Mg-11.3Gd-2.5Zn-0.7Zr	As-extruded	0.17	–	114

Microstructure

Besides alloying, the microstructure can be further tailored to meet the requirements of orthopaedic applications by adjusting the grain size, second phases and their distribution, twins, texture etc. Different processing techniques, such as heat treatment and thermo-mechanical processing, can be applied to achieve this.

Grain size

The corrosion behaviour of Mg alloys is closely related to their grain size. Grain refinement is an effective way to improve the corrosion performance of Mg alloys.[48, 119-122] For example, Lu et al.[111] found that the bio-corrosion rate of Mg-3Zn-0.3Ca is a function of grain size and the volume fraction of secondary phase. Birbilis et al.[122] proposed that the corrosion rate increases as the logarithm of average grain size increases in pure Mg. Ralston et al.[123] also described a relationship between corrosion rate and grain size: $i_{corr}=(A)+(B)\cdot GS^{-0.5}$ (where A is a constant and a function of the environment; B is a material constant and is determined by the composition and impurity level of the material; *GS* is grain size and i_{corr} is the corrosion rate). Corrosion resistance can be linearly enhanced by reducing the grain size. It has been reported that the reason why grain refinement causes a decreased corrosion rate is because of the improved passive film.[124, 125] A high grain boundary density promotes a better oxide film conduction rate on surfaces with low to passive corrosion rates and therefore a fine grain structure is more corrosion resistant. Song and StJohn [126] indicated that the skin of the die-cast AZ91D alloy exhibits better corrosion performance than the interior, because of the more continuous $Mg_{17}Al_{12}$ phase formed around finer α-Mg grains. If the grains are small and the volume fraction of the $Mg_{17}Al_{12}$ phase is not too low, then the $Mg_{17}Al_{12}$ phase forms continuously like a net, and is difficult to undercut because corrosion development cannot easily progress through numerous $Mg_{17}Al_{12}$ precipitates. The $Mg_{17}Al_{12}$ phase is exposed and the α-Mg phase corrodes preferentially. Eventually, the final surface of the sample has large amounts of $Mg_{17}Al_{12}$ which are more corrosion resistant than the α-Mg phase, thus the corrosion resistance is enhanced.[91, 127]

Second phase

Second phases have a significant impact on the performance of Mg alloys.[128, 129] A homogenous microstructure is desirable, because a difference in corrosion potential between the α-Mg and the second phase causes micro-galvanic corrosion. In AZ alloys, the $Mg_{17}Al_{12}$ phase (–1.20 V) is nobler than the α-Mg matrix (–1.65 V)[46] and therefore acts as a cathode and aggravates the corrosion of Mg.[91, 130] Some researchers have proposed that the $Mg_{17}Al_{12}$ phase can act as a corrosion barrier and have a positive effect on corrosion resistance.[128, 129, 131] The fraction and distribution of $Mg_{17}Al_{12}$ phases are important

factors in determining which effect dominates. A finely- and continuously-distributed β-phase serves as a corrosion barrier and inhibits corrosion;[119] otherwise, the β-phase promotes corrosion. Song et al.[126] proposed that more continuous second phases can benefit the corrosion resistance of the Mg-RE-Zr alloy (MEZ alloy). The morphology of the second phase also affects the corrosion behaviour of Mg alloys. Srinivasan et al.[132] reported that Mg with a coarse Chinese script Mg_2Si phase shows a weaker corrosion performance than that with evenly-distributed polygonal-shaped Mg_2Si phases. The reduction and refinement of Mg_2Si phases also lead to better corrosion behaviour of Mg-Si(-Ca) alloys.[91] The rod-shaped nano-scale β'_{www1} precipitates which form during aging strengthen the Mg-3Zn alloy, but decrease its corrosion resistance.[101] Mao et al.[133] have reported that different thermal–mechanical processing treatments result in differences in mechanical and bio-corrosion performance. The yield strength (YS), ultimate tensile strength (UTS) and elongation of Mg-3.1Nd-0.2Zn-0.4Zr (JDBM) alloy significantly improved after hot extrusion, thanks mainly to precipitation strengthening.[94, 134] The corrosion rate of extruded JDBM (0.13 mm/year) was much lower than that of AZ91 (1.02 mm/year), because of a homogeneous distribution of nano-scaled Mg12Nd phase.[135] Mg-2.2Nd-0.1Zn-0.4Zr (JDBM-2) alloy after double extrusion showed a high strength (276 MPa) and elongation (34%) and a good corrosion rate (0.37 mm/year) in artificial plasma for 120 hours, caused by the presence of nanoparticles and by grain refinement.[133] The finely dispersed nano-scale precipitates not only improve the mechanical properties but also lead to homogeneous degradation and a reduced corrosion rate.

Other factors

Several researchers report that twins, texture and dislocations all have influences on the corrosion performance. Aung and Zhou[120] reported that the existence of twins can accelerate the corrosion of Mg alloys. After equal channel angular extrusion, a higher density of dislocations and twins appeared and a more severe dissolution of the anode resulted.[121] Andrei et al.[136] reported that the equilibrium potential in the vicinity of the dislocations is locally reduced, thus causing accelerated dissolution of the anode. According to Xin et al.[137] extruded AZ31 sheet showed better corrosion resistance because of the initial basal texture. Schmutz et al.[138] reported that filaments of corrosion propagated at twin boundaries; this corrosion took place on a plane near the basal plane and then propagated down the prismatic planes.

In order to meet the biomedical requirements of Mg alloys, therefore, a desirable microstructure needs to be achieved: refined grains increasing strength and ductility, a homogenous distribution of second phase resulting in homogenous bio-corrosion, a reduced density of boundaries (such as twin boundaries) limiting the propagation of corrosion and a small-scaled second phase reducing galvanic corrosion.

Novel structure development

So far we have been describing traditional monolithic metallic alloy components. There are, however, more adventurous possibilities which may have a significant impact on implanted components.

Glassy structures

Mg-based BMGs display a uniform corrosion performance due to their single phase structure and chemical homogeneity. An increased corrosion resistance, uniform corrosion morphology and better cytocompatibility of $Mg_{66}Zn_{30}Ca_4$ BMG have been reported by Gu et al.[139] The glassy $Mg_{60+x}Zn_{35-x}Ca_5$ ($0 \le x \le 7$) alloys exhibited a distinct reduction in hydrogen evolution.[140] A wide range of *in vitro* electrochemical corrosion rates of BMGs has been shown, for example 11.2 $\mu A/cm^2$ for $Mg_{70}Zn_{25}Ca_5$[139] and 0.02 $\mu A/cm^2$ for $Mg_{65}Cu_{20}Y_{10}Zn_5$.[141] The $Mg_{67}Zn_{28}Ca_5$ BMG shows good tensile strength: 675–894 MPa,[142] while the $Mg_{66}Zn_{30}Ca_4$ BMG shows good compressive strength: 716–854 MPa.[140] However, the manufacturability and application of BMGs is limited by their glass-forming ability which is very sensitive to the fabrication methods and the purity of the components. Moreover, the brittleness of BMGs needs to be carefully considered: they normally fail without, or with limited, macro-plasticity. Nevertheless, significant elongations of BMGs have been reported: 1.6% for $Mg_{65}Cu_{15}Ag_{10}Y_2Gd_8$,[143] 0.5% for $Mg_{63}Cu_{16.8}Ag_{11.2}Er_{10}$[144] and 0.9% for $Mg_{65}Cu_{7.5}Ag_5Ni_{7.5}Gd_5$.[143] The structural relaxation at 20°C and 37°C for $Mg_{95-x}Zn_xCa_5$ BMG has been examined. The relaxation time increased from 10 to 30 days at 20°C, combined with a dramatic reduced hydrogen evolution.[145] Yu et al.[146] reported that the addition of Yb (2at% and 4at%) significantly improved the ductility of MgZnCa BMGs.

The fabrication method and processing parameters significantly affect the alloying composition and microstructure of Mg-based BMGs. The current development of Mg-based BMGs for clinical applications is still focused on the forming ability and formation mechanism. A simple fabrication process and production of reasonably large sized BMGs need to be further developed. It has been reported that Mg-based BMGs have higher yield stress than their crystalline counterparts due to the absence of the crystallographically-defined slip systems in polycrystalline metallic materials.[147] However the ductility of Mg-based BMGs needs to be further improved because they are extremely brittle. In addition, while some Mg-based BMGs possess good biocompatibility, other Mg-based BMGs contain toxic alloying elements (such as transition metals and RE elements) because of their good glass-forming ability. Thus the alloying design of Mg-based BMGs needs to be carefully tailored.

Composite structures

Mg MMCs show a wide range of mechanical and corrosion behaviours because of the wide range of reinforcements and their content, distribution and size. The manufacturing methods are usually powder metallurgy or stir casting. The matrix materials are biomedical Mg alloys such as Mg-Ca, Mg-Al, Mg-Zn and Mg-RE. Calcium phosphate-based ceramics (like calcium polyphosphate, hydroxyapatite and tri-calcium phosphate), calcium, bioactive glass and zinc oxide have all been used to reinforce Mg MMCs. The amount, distribution and size of reinforcements are very important for the mechanical and bio-corrosion properties of Mg MMCs. For example, fluorapatite nanoparticles (up to 20%) have been used to improve the mechanical properties of AZ91/FA MMC.[148]

Mg/ZnO MMCs (20wt% ZnO nanoparticles) have been prepared using powder metallurgy and confer improved tensile strength, hardness and corrosion resistance but with reduced elongation.[149] ZK60/CPP (calcium polyphosphate particles) MMCs have been produced with a compressive strength of 495 MPa.[150] Gu et al.[151] developed Mg-hydroxyapatite (10wt%, 20wt% and 30wt%) composites using powder metallurgy. Mg/10HA composites showed higher YS, lower UTS and elongation, reduced corrosion resistance and no toxicity. An MMC was fabricated using Mg-2.9Zn-0.7Zr as the matrix and 1wt% nano HA particles as reinforcement; it had a corrosion rate of 0.75 mm/year.[152] A nano-sized β-tricalcium phosphate/Mg-3Zn-Ca composite was produced and showed a UTS of 125 MPa and elongation of 2.85%.[153] Poly (L-lactic) acid-$Mg_{65}Zn_{30}Ca_5$ composites were studied as potential orthopaedic implant candidates; they showed high corrosion resistance and good antibacterial properties.[154] A collagen (10%)-hydroxyapatite (80%)-Mg (10%) composite scaffold was developed as a bone substitute and showed favourable bone healing and regeneration.[155] A novel Mg nanocomposite scaffold was fabricated and demonstrated that a Mg cationic microenvironment promotes cell viability and osteogenic differentiation properties *in vitro* leading to effective bone defect repair.[156, 157]

Mg-based composites can provide combined properties. For example, composites made of bioactive ceramics can claim two important features: mechanical strength and bioactivity. Currently, calcium phosphate ceramics are mainly used for bone defect filling (in dental and orthopaedic surgery). Hydroxyapatite is adopted to enhance the bonding of hip joint prostheses because of excellent biological behaviour, lack of inflammation and the absence of fibrous immunological reactions.

In summary, the strength and elongation of currently-studied Mg-based composites need to be further improved. As things stand at the moment, the alloying/reinforcement needs to be further optimised to satisfy the requirements for practicable orthopaedic implants.

Porous structures

Porous implants (also called scaffolds) are under the spotlight for orthopaedic applications, because their interconnected pore structure encourages tissue ingrowth and survival of the vascular system required for continuing bone development.[158, 159] Such interconnected pore networks facilitate the delivery of oxygen and nutrients to the cells and the removal of products stemming from cell metabolism and from degradation of the scaffold.[160, 161] Moreover, the material's modulus can be controlled via the porosity, which enables the design of implant materials with a modulus close to that of human bone.[162] Other mechanical properties of Mg scaffolds can also be adjusted by changes to the porosity and pore size.[163] Razavi et al.[164] have specifically proposed that Mg-based alloys can be employed as biocompatible, bioactive, and biodegradable scaffolds for orthopaedic applications.

Powder metallurgy, laser additive manufacturing, the metal/gas eutectic unidirectional solidification process and the negative salt-pattern moulding method have all been used to produce a porous Mg scaffold. Porous WE43 scaffolds were fabricated by laser-powder bed fusion and their *in vitro* performance was first reported by Li et al.[165] The diamond lattice was adopted to construct a porous scaffold cylinder with a diameter of 10 mm and a height of 11.2 mm, as shown in **Figure 6A**. Geng et al.[166] reported that the pore size and porosity (48%) of a honeycomb-structured Mg scaffold (shown in **Figure 6B**[167]) can be controlled by the laser perforation technique. Witte et al. reported an open porous AZ91 alloy scaffold with porosity ranging from 72% to 76% and a pore size varying between 10 and 1000 μm, which was created by infiltrating molten Mg into a NaCl preform and then washing out the salt preform in NaOH solution.[40, 168] Gu et al.[169] produced a lotus-type porous pure Mg using a metal/gas eutectic unidirectional solidification method, which showed a slower decay in compressive YS than that of pure Mg during immersion in simulated body fluid.

It has been stated that the scaffold structure provides three-dimensional space for cell adhesion and ingrowth, giving good biocompatibility.[170] More importantly, the laser additive manufacturing technology used to build the scaffold has significant advantages in the fabrication of complex porous structures and customised implants addressing specific clinical needs. However, the pore structure (including pore size, shape, connectivity, etc.) needs to be carefully controlled, because this is one of the key factors determining the mechanical properties of porous Mg.

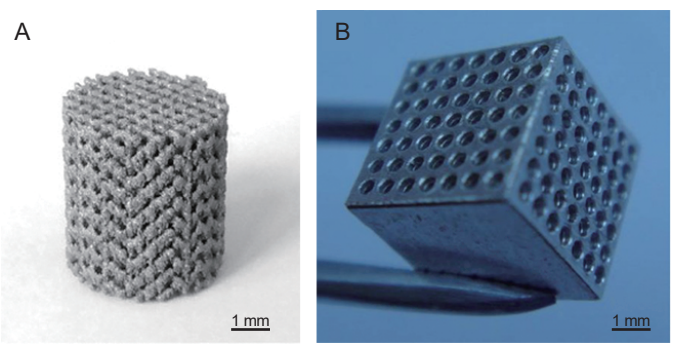

Figure 6. (A) As-built WE43 scaffold with diamond lattice fabricated by selective laser melting. Reprinted from Li et al.[40] Copyright 2017, with permission from Acta Materialia Inc. (B) Honeycomb-structured magnesium scaffold produced by laser perforation. Reprinted from Tan et al.[167] Copyright IOP Publishing. Reproduced with permission. All rights reserved. Scale bars: 1 mm.

Besides the traditional techniques such as melting and casting, other fabrication methods have been developed to obtain biomedical Mg implants, including powder metallurgy, metallic glass forming and laser additive manufacturing. The different fabrication processes directly affect the microstructure and relevant biological performance, mechanical properties and bio-corrosion behaviour.[118, 171] In particular, the accurate regulation of alloying elements, microstructure design, biocompatibility tailoring, machinability and precise control of porous structure need to be considered and further investigated. Moreover, the *in vitro* and *in vivo* testing needs to be carefully studied.

Performance Testing

Mechanical testing

A tensile test machine with tensile grips and extensometer can be obtained to measure the characteristics of alloys. Tensile tests are simple, inexpensive and standardised and measure the YS, UTS and elongation. Results from tensile testing can be used for material comparison, quality control and alloy development. Standard tensile tests can follow ASTM B557[172] and ISO 6892-1.[173] In clinical applications the Mg implant is continuously under the load in a physiological environment. Fatigue-corrosion testing is also necessary because of the specific requirements of orthopaedic applications. Here the ASTM testing standard WK61103[174] can be employed.

In vitro testing

In vitro experiments are convenient and can provide quick and reasonable feedback on efficacy as compared with *in vivo* testing. The simulated body fluid method is popular; it is an aqueous solution with ion concentrations and pH value equal to those of human body fluids. The corrosion of Mg in simulated body fluid increases the pH because of alkalisation, which affects the biodegradation rate. In order to minimise the pH variation of simulated body fluid, the solution needs to be refreshed every 24 hours and the ratio of sample surface to the volume of solution kept high. **Table 6** shows several solutions used in *in vitro* tests.[175]

Table 6. The concentration of ions and pH values in blood plasma and in different solutions.

Ion	Blood plasma	Ringer's solution	Earle's balanced salt solution	Hank's balanced salt solution	Kokubo's simulated body fluid
Na^+ (mM)	142.00	130.00	143.60	138.00	142.00
K^+ (mM)	5.00	4.00	5.37	6.14	5.00
Ca^{2+} (mM)	2.50	1.40	1.80	1.26	2.50
Mg^{2+} (mM)	1.50	NA	0.81	0.81	1.50
Cl^- (mM)	103.00	109.00	125.30	144.8	147.80
HCO_3^- (mM)	27.00	NA	26.2	4.2	4.20
HPO_4^{2-} (mM)	1.00	NA	1.00	0.78	1.00
SO_4^{2-} (mM)	0.50	NA	0.81	0.81	0.50
Ca/P (mM)	2.50	NA	1.80	1.62	2.50
Buffer (mM)	NA	NA	NA	NA	Tris
pH	7.4	6.5	6.7–6.9	6.7–6.9	7.4

Note: NA: not applicable. Data are from Gu et al.[147]

Several methods are used to measure the degradation rates of Mg alloys: mass loss, hydrogen evolution, electrochemical techniques and micro-computed tomography measurement.

1) Mass loss is the simplest method for degradation testing, with mass loss rates depending on the test duration. The degradation rate determined by mass loss can be calculated using the following equation.

$$\text{degradation rate (mm/year)} = \frac{k \times \text{weight change}}{\text{surface area} \times \text{immersion time} \times \text{density}} \quad (6)$$

(k is a constant, 8.76×10^4)

The tested Mg specimen is placed in the corrosion medium for a period of time, at the end of which the Mg alloy is taken out and washed with a cleaning solution (such as dilute chromic acid) to remove all corrosion products and then the resultant mass change is measured. This classic method has been used by a number of researchers.[117, 176-181]

2) A hydrogen evolution method has been developed by Song et al.[182] based on the collection of hydrogen gas during degradation of Mg in aqueous solutions. The hydrogen evolution measurement is currently very popular and is widely accepted by many researchers.[10, 42, 59, 106, 107, 178-181] The mechanism of this measurement is simple and easy to understand, and is based on the reaction below:

$$Mg + 2H_2O \rightarrow Mg(OH)_2 + H_2\uparrow \quad (7)$$

The evolution of one mole of hydrogen gas corresponds to the dissolution of one mole of Mg metal. Thus, the volume of evolved hydrogen gas is equal to the weight loss of the alloys, and they can be converted into the same units (mm/year).

3) Electrochemical measurement is widely used to measure the *in vitro* degradation behaviour of Mg alloys.[106, 148, 183-185] The greatest advantage is that it can be used to obtain the real-time corrosion rate. Changes in corrosion behaviour can be instantaneously observed. Generally, the Mg sample is used as the working electrode, platinum as the counter electrode and a saturated calomel electrode as the reference electrode. Using this method, more corrosion information can be accessed, such as the relative rates of the anodic and cathodic reactions over a range of potentials.[186] A number of investigations indicate that the corrosion rate of Mg alloys measured by electrochemical testing agrees with that by hydrogen evolution and helps to

increase the understanding of how corrosion takes place.[119, 186, 187]

4) Micro-computed tomography (a non-destructive technique) has been demonstrated to be a powerful technique to monitor *in vitro* degradation.[105, 188-190] The evaluation of the bio-corrosion rate depends on a comprehensive observation of the Mg specimen before and after immersion testing. The volume losses of the samples can be calculated and then converted to the same units (mm/year). Lu et al.[105] reported the corrosion morphology and degradation rate of Mg-3Zn-0.3Ca alloys using three-dimensional reconstructions, as shown in **Figure 7**. The as-cast Mg-3Zn-0.3Ca has been severely attacked by corrosion and has lost 34.3% of its initial volume.

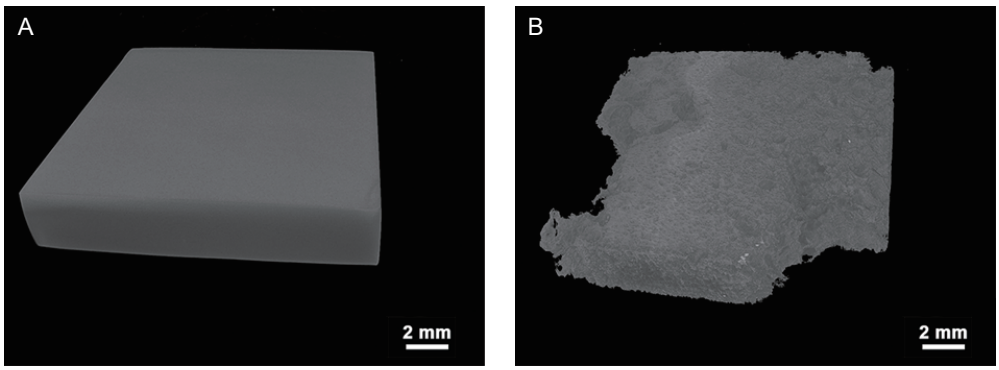

Figure 7. Micro-computed tomographic three-dimensional images of as-cast Mg-3Zn-0.3Ca alloy. (A) Before immersion test. (B) After immersion test. Scale bars: 2 mm. Reprinted from Lu et al.[105] Copyright 2018, with permission from Acta Materialia Inc.

***In vivo* testing**

The *in vivo* assessment of the compatibility of biomaterials and medical devices with tissue is important for the development and implementation of implants for human use. Many *in vivo* studies have been conducted to understand the degradation process and the associated mechanisms. Animal models are adopted in order to determine the response to the biomaterials or medical devices, such as the interactions of various cell types with the implants, endocrine factors acting on cells around the implant and interactions with blood-borne cells and proteins. *In vivo* studies have mainly been performed on small animals, such as guinea pigs, rats and rabbits. Heublein et al.[191] investigated a cardiovascular stent (AE21 alloy) in domestic pigs. There is a report describing the implantation of Mg chips into the spines of sheep.[192] The first comprehensive *in vivo* study on Mg alloys was carried out by Witte et al.[39] on four different Mg alloys (AZ31, AZ91, WE43 and LAE442), and these four Mg alloys were implanted into the femurs of guinea pigs. A newly-formed mineral phase was observed on the surface of the Mg implants during implant degradation, which stained with calcein green under fluorescent light (**Figure 8A**).[39] The *in vivo* bio-corrosion morphology of the remaining Mg alloy in the guinea pig femora is shown in **Figures 8B** and **C**.[109] It can be seen that the AZ91D rod was almost completely corroded, while the LAE442 rod was corroded more uniformly. Both of these Mg alloys exhibited good biocompatibility as evidenced by the direct contact with newly-formed bone.

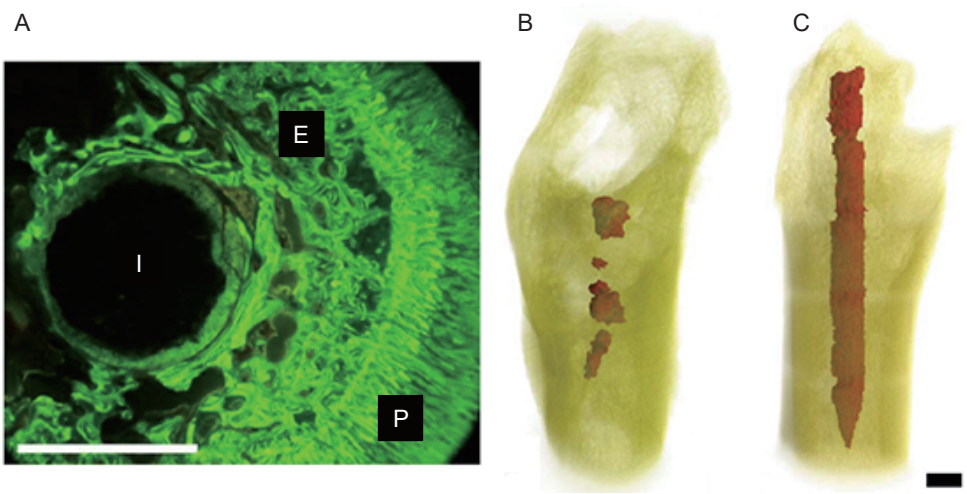

Figure 8. (A) Fluoroscopic image of cross-section of magnesium rod in a guinea pig femur. E: endosteal bone formation; I: implant residual; P: periosteal bone formation. (B) Three-dimensional reconstruction of remaining AZ91D in the femur of a guinea pig. (C) Three-dimensional reconstruction of remaining LAE442 in the femur of a guinea pig. Scale bars: 1.5 mm. A–C were reprinted from Witte et al.[39, 109] Copyright 2005 & 2006, with permission from Elsevier Ltd.

Recently, some *in vivo* studies were carried out on large animal models. A goat was used to study the clinical capability of osteosynthesis of a lean Mg alloy (Mg-0.45Zn-0.45Ca) screw.[51] *In vivo* transformation experiments on high-purity weight-bearing Mg screws were also carried out on goats.[193] Small animals (rats) and large animals (sheep) have been used to compare the biodegradation rate, bone formation and in-growth of bone into Mg-0.45Zn-0.45Ca implants.[194] A pig model was designed to evaluate the *in vivo* performance of a Mg-4Zn-0.1Sr anastomosis ring.[195] A miniature pig has been employed to perform pre-clinical testing of human-sized Mg implants at multiple implantation sites.[196]

Cytotoxicity

Cytotoxicity testing is one of the biological evaluation and screening tests that uses tissue cells *in vitro* to observe the effects of medical implants on cell growth, reproduction and morphology.[197] It is an important indicator for quickly evaluating the biocompatibility of implants because it is fast, simple and highly sensitive. Three types of cytotoxicity test are specified in ISO 10993:[198] extract, direct contact and indirect contact tests. The extract test is suitable for evaluating the toxicity of soluble substances released from implants. The direct contact test is the most sensitive and can be used to measure even weak cytotoxicity.[199] The indirect contact test is used on implants with high toxicity and/or small molecular weight.[200, 201] Bone marrow-derived mesenchymal stromal cells, murine fibroblast cells (L-929) and murine calvarial preosteoblasts (MC3T3-E1) are commonly used for cytotoxicity studies.[202-207] The cytotoxicity assay includes cell adhesion, cell viability and proliferation assessments. Cell morphology can be viewed by fluorescence staining under an inverted fluorescence microscope. In order to investigate cell adhesion, samples seeded with MC3T3-E1 pre-osteoblasts were rinsed with phosphate-buffered saline (PBS).[207] MC3T3-E1 cells were directly seeded onto Mg alloy to study the cell proliferation behaviour.[208] A standard MTT assay was adopted to measure cell viability.[202]

The degradation rate of Mg alloys determines the ion release rate in the physiological environment. The amount of released elements significantly affects the biocompatibility of the Mg alloys. An evaluation of the biosafety of Mg implants must be performed. Currently, preparation of the extracts from medical devices for cytotoxicity testing needs to follow Parts 5 and 12 of ISO 10993.[198, 209] However, Mg alloys can react with an aqueous environment, release Mg ions and produce a higher pH value and osmolality in the surrounding medium,[186] which is significantly affected by the constituents of the medium.[210] In order to mimic an *in vivo* environment, a cell culture medium supplemented with serum is recommended.[211] Wang et al.[212] proposed a modified cytotoxicity testing standard for biodegradable Mg-based materials: a minimum 6-fold to a maximum 10-fold dilution of extracts from Mg implants for cytotoxicity tests. It has been reported that the test conditions can significantly influence the cytotoxicity testing of biodegradable metallic materials, which further suggested that the test conditions need to be carefully specified and different studies need to be cautiously compared.[213]

Future Perspectives

Mg is an essential ion in metabolism and can encourage bone growth, which helps the proper fixation of an implant into the host bone and potentially allows full healing of bone defects after degradation.[186, 214] Importantly, biomaterials need to be designed to be bioactive and/or bioresorbable to improve tissue growth. Therefore, a biodegradable Mg alloy with great biocompatibility can make an ideal implant for load-bearing orthopaedic applications. Complex and/or customised shapes consistent with specific patient needs are required in real clinics nowadays. Thus, additive manufacturing is assuming greater and greater importance for implant manufacture, including for Mg. In addition, the influence of local pH changes on the adjacent tissue, evolution of hydrogen gas and the concentration of released metallic ions caused by bulk Mg-based implants can be reduced by adopting Mg scaffolds due to the smaller volume of implant. Furthermore, a material with porosity changing across the volume (a functionally-graded material) is currently believed to improve osseo-integration.[215] This can be achieved by an additively-manufactureld scaffold. These unique features suggest that additively-manufactureld Mg scaffolds with bone-mimicking characteristics will become promising orthopaedic implants, possessing sufficient mechanical strength and ductility, low elastic modulus, excellent biocompatibility, and a complex shape.

Over recent decades, new types of biodegradable Mg alloys have mainly been developed by casting because it is easy to regulate the alloying elements. However casting generally leads to large grains, which need subsequent deformation (such as extrusion, rolling and forging) to reduce their size. In particular, severe plastic deformation has been widely used to obtain fine grains and therefore further tailor the mechanical and corrosion performance. In contrast, additive manufacturing involves rapid melting and solidification which results directly in a fine microstructure. This technique also shows an ability to regulate the second phase distribution and composition, because the alloy elements mainly dissolve in the matrix due to the fast advanced solid/liquid frontier ('solute capture effect').[216] The reduced second phase caused by the extended solid solution of alloying elements may result in improved corrosion resistance because of the reduced galvanic corrosion effect.

However, it needs to be noticed that the additive manufacturing of Mg is still challenging. Unlike Ti or Fe alloys, the melting point (~650°C) of Mg is quite close to its boiling point (~1091°C) which limits the range of process parameters. In addition, Mg is easily ignited during laser processing, because of its low boiling point, high vapour pressure, low surface tension and density. The formability of Mg is hard to control because it is easily oxidised due to its active chemical properties. The densification of Mg (reduction of processing pores) needs to be improved to enhance the formability. Therefore, the fundamental mechanisms of processing as it affects the fabricability of Mg need to be further studied, like its residual stress control, processing stability, interaction between laser beam and Mg, internal defect formation mechanism and so on.

Alloying is still the critical factor determining the

biocompatibility, mechanical properties and biodegradation behaviour of orthopaedic implant materials. Firstly, the toxicity of alloying elements in the biological environment needs to be carefully considered. Some nutrient alloying elements are good candidates. For example, Zn is recognised as a nutritionally-essential element in the human body. Ca is a major component of human bone and is an important element in cell signalling; released ions are beneficial for bone healing.[217] Sr belongs to Group IIA of the periodic table (the same as Mg) and shares similar chemical, biological and metallurgical properties, which can stimulate bone cell differentiation and inhibit bone resorption.[218] Zr is known to be of low toxicity to living organisms and to have a stimulating effect on bone cells, which can improve bone integration.[219]

Secondly, in order to achieve suitable mechanical properties (UTS: ~200 MPa, elongation: ~20%) and service life-time (3–4 months for orthopaedic application),[133] the alloying design, processing history, heat treatment and impurity control (like Fe, Ni, Cu and Co) need to be carefully considered and tailored properly. For orthopaedic applications, the fatigue-corrosion behaviour in an aqueous environment also must be taken into account. The mechanical properties can be improved by various strengthening mechanisms, such as grain refinement strengthening, solid solution strengthening and precipitate strengthening.

Thirdly, for bone implants, 3–4 months is required from fracture callus formation to new bone formation and eventually solid bone healing to restore most of the bone's original strength. For example, when the dimensions of a locking compression plate (locking compression plate 3.5–423.621 from Depuy Synthes[220]) are 163 mm × 10 mm × 2 mm (volume of 3.84 cm^3 determined by micro-computed tomography), the degradation rate needs to be controlled to be below 0.97 mm/year which would correspond to complete degradation in 3 months according to equation (6). The biodegradation properties can be tailored by adjusting the alloying treatment, grain refinement, the formation of a passivation film, reduction in the cathode–anode potential difference and secondary phase amount and distribution. The elements Nd and Y are good candidates which can significantly improve the mechanical performance of Mg alloys by grain refinement strengthening, solid solution strengthening and precipitate strengthening.[221] They also can greatly decrease the corrosion rate by removing impurities, creating less noble intermetallic phases ('scavenger effect' on impurities) and forming stable protective films.[222] However the concentrations of Nd and Y need to be carefully controlled below the threshold level (e.g. < 5wt% depending on the actual component).

Currently, some Mg alloys such as WE43,[165, 223] AZ91,[224] Mg-9wt% Al[225] and ZK60[226-228] are fabricated using laser additive manufacturing. The *in vitro* static degradation behaviour has been studied.[165, 226, 229, 230] However, the *in vivo* response, especially the dynamic biodegradation including geometric and mechanical changes, have been barely reported. The dynamic degradation of Mg leads to varied biological interactions and mechanical performance. Therefore, the dynamic evolution of Mg implants in the physiological environment needs to be investigated, including changes in the implant shape, variations in the mechanical strength and elastic modulus, pH variation, the release of corrosion products, the amount of released metallic ions, hydrogen gas and the changed biocompatibility. In addition, the related modelling, which can accurately simulate the dynamic physiological–chemical–mechanical variation during the biodegradation process along with bone healing, needs development.

In summary, the following aspects are in the spotlight for designing the next generation of biodegradable Mg-based alloys for orthopaedic applications: 1) Mg-based alloys with excellent biocompatibility, especially incorporating nutrient elements (such as Ca, Zn, or Sr) along with controlling elements such as Nd and Y below the threshold level; 2) development of novel fabrication techniques to satisfy the complex shape and various size requirements, for example additive manufacturing, to build the best processing window (suitable selection of processing parameters); 3) innovative three-dimensional model design with changing porosity across the volume, resulting in a superior ability of Mg implants to mimic bone/tissue growth); 4) mathematical modelling and simulation, which can predict the dynamic mechanical and biodegradation variation of a Mg implant during implantation; and 5) effective application of *in vivo* testing on the basis of initial *in vitro* evaluation, finally translating to safe clinical application.

Author contributions
Concepts, literature search, statistical analysis and manuscript preparation: YL; manuscript editing: YL, IPJ; manuscript review: SD, IPJ, YLC. All authors discussed the results and contributed to the final manuscript.
Financial support
None.
Acknowledgement
None.
Conflicts of interest statement
The authors declare that they have no known competing financial interests or personal relationships that could have appeared to influence the work reported in this paper.

1. Ratner, B. D.; Hoffman, A. S.; Schoen, F. J.; Lemons, J. E. *Biomaterial sciences: an introduction to materials in medicine*. Academic Press: San Diego. **1996**.
2. Temenoff, J. S.; Mikos, A. G. *Biomaterials: the intersection of biology and materials sceince*. Pearson. **2008**.
3. Zheng, Y. F.; Gu, X. N.; Witte, F. Biodegradable metals. *Mater Sci Eng R Rep*. **2014**, *77*, 1-34.
4. B. Ermanno. Basic Composition and Structure of Bone. In *Mechanical testing of bone and the bone-implant interface*, An, Y. H.; Draughn, R. A., eds.; CRC Press: *Boca Raton*, **1999**; pp 3-22.
5. Suzuki, H.; He, J. Evaluation on bending properties of biomaterial GUM Metal meshed plates for bone graft applications. In IOP Conference Series: Materials Science and Engineering, IOP Publishing: *Tianjin*. **2017**; Vol. 269, p 012078.

6. Augat, P.; von Rüden, C. Evolution of fracture treatment with bone plates. *Injury.* **2018**, 49 *Suppl 1*, S2-S7.
7. Nana, A. D.; Joshi, A.; Lichtman, D. M. Plating of the distal radius. *J Am Acad Orthop Surg.* **2005**, *13*, 159-171.
8. AO Foundation. AO Foundation Surgery Reference. https://surgeryreference.aofoundation.org/. Accessed April 13, 2021.
9. Gueorguiev, B.; Lenz, M. Why and how do locking plates fail? *Injury.* **2018**, *49 Suppl 1*, S56-S60.
10. Perren, S. M. Evolution of the internal fixation of long bone fractures. The scientific basis of biological internal fixation: choosing a new balance between stability and biology. *J Bone Joint Surg Br.* **2002**, *84*, 1093-1110.
11. Bastias, C.; Henríquez, H.; Pellegrini, M.; Rammelt, S.; Cuchacovich, N.; Lagos, L.; Carcuro, G. Are locking plates better than non-locking plates for treating distal tibial fractures? *Foot Ankle Surg.* **2014**, *20*, 115-119.
12. Hsu, K. L.; Kuan, F. C.; Chang, W. L.; Liu, Y. F.; Hong, C. K.; Yeh, M. L.; Su, W. R. Interlocking nailing of femoral shaft fractures with an extremely narrow medullary canal is associated with iatrogenic fractures. *Injury.* **2019**, *50*, 2306-2311.
13. Cronier, P.; Pietu, G.; Dujardin, C.; Bigorre, N.; Ducellier, F.; Gerard, R. The concept of locking plates. *Orthop Traumatol Surg Res.* **2010**. doi: 10.1016/j.otsr.2010.03.008.
14. McRae, R.; Esser, M. *Practical Fracture Treatment.* 5th ed. Churchill Livingstone: 2008.
15. Elias, C. N.; Lima, J. H. C.; Valiev, R.; Meyers, M. A. Biomedical applications of titanium and its alloys. *JOM.* **2008**, *60*, 46-49.
16. ASTM F67. Standard specification for unalloyed titanium, for surgical implant applications. **2006**.
17. ASTM F138-19. Standard specification for wrought 18chromium-14nickel-2.5molybdenum stainless steel bar and wire for surgical implants. **2020**.
18. ASTM F1537-20. Standard specification for wrought cobalt-28chromium-6molybdenum alloys for surgical implants. **2020**.
19. Disegi, J. A.; Eschbach, L. Stainless steel in bone surgery. *Injury.* **2000**, *31 Suppl 4*, 2-6.
20. Disegi, J. A. Titanium alloys for fracture fixation implants. *Injury.* **2000**, *31 Suppl 4*, 14-17.
21. Golish, S. R.; Mihalko, W. M. Principles of biomechanics and biomaterials in orthopaedic surgery. *Instr Course Lect.* **2011**, *60*, 575-581.
22. Bayraktar, H. H.; Morgan, E. F.; Niebur, G. L.; Morris, G. E.; Wong, E. K.; Keaveny, T. M. Comparison of the elastic and yield properties of human femoral trabecular and cortical bone tissue. *J Biomech.* **2004**, *37*, 27-35.
23. Ryan, G.; Pandit, A.; Apatsidis, D. P. Fabrication methods of porous metals for use in orthopaedic applications. *Biomaterials.* **2006**, *27*, 2651-2670.
24. Vamsi Krishna, B.; Xue, W.; Bose, S.; Bandyopadhyay, A. Engineered porous metals for implants. *JOM.* **2008**, *60*, 45-48.
25. Lhotka, C.; Szekeres, T.; Steffan, I.; Zhuber, K.; Zweymüller, K. Four-year study of cobalt and chromium blood levels in patients managed with two different metal-on-metal total hip replacements. *J Orthop Res.* **2003**, *21*, 189-195.
26. Maehara, T.; Moritani, S.; Ikuma, H.; Shinohara, K.; Yokoyama, Y. Difficulties in removal of the titanium locking plate in Japan. *Injury.* **2013**, *44*, 1122-1126.
27. Morgan, E. F.; Unnikrisnan, G. U.; Hussein, A. I. Bone mechanical properties in healthy and diseased states. *Annu Rev Biomed Eng.* **2018**, *20*, 119-143.
28. Friedrich, H. E.; Mordike, B. L. *Magnesium technology: metallurgy, design data, applications.* Springer, Berlin, Heidelberg, 2006.
29. Schweitzer, P. E. Metallic materials: physical, mechanical, and corrosion properties. CRC Press: 2020.
30. Staiger, M. P.; Pietak, A. M.; Huadmai, J.; Dias, G. Magnesium and its alloys as orthopedic biomaterials: a review. *Biomaterials.* **2006**, *27*, 1728-1734.
31. Park, J. B. *Biomaterials science and engineering.* Plenum Press: New York,1984.
32. Hartwig, A. Role of magnesium in genomic stability. *Mutat Res.* **2001**, *475*, 113-121.
33. Okuma, T. Magnesium and bone strength. *Nutrition.* **2001**, 17, 679-680.
34. Song, G.; Song, S. A possible biodegradable magnesium implant material. *Adv Eng Mater.* **2007**, *9*, 298-302.
35. Rodríguez-Sánchez, J.; Pacha-Olivenza, M. Á.; González-Martín, M. L. Bactericidal effect of magnesium ions over planktonic and sessile Staphylococcus epidermidis and Escherichia coli. *Mater Chem Phys.* **2019**, *221*, 342-348.
36. Xu, L.; Yu, G.; Zhang, E.; Pan, F.; Yang, K. In vivo corrosion behavior of Mg-Mn-Zn alloy for bone implant application. *J Biomed Mater Res A.* **2007**, *83*, 703-711.
37. Saris, N. E.; Mervaala, E.; Karppanen, H.; Khawaja, J. A.; Lewenstam, A. Magnesium. An update on physiological, clinical and analytical aspects. *Clin Chim Acta.* **2000**, *294*, 1-26.
38. Gu, X.; Zheng, Y.; Cheng, Y.; Zhong, S.; Xi, T. In vitro corrosion and biocompatibility of binary magnesium alloys. *Biomaterials.* **2009**, *30*, 484-498.
39. Witte, F.; Kaese, V.; Haferkamp, H.; Switzer, E.; Meyer-Lindenberg, A.; Wirth, C. J.; Windhagen, H. In vivo corrosion of four magnesium alloys and the associated bone response. *Biomaterials.* **2005**, *26*, 3557-3563.
40. Witte, F.; Ulrich, H.; Rudert, M.; Willbold, E. Biodegradable magnesium scaffolds: Part 1: appropriate inflammatory response. *J Biomed Mater Res A.* **2007**, *81*, 748-756.
41. Claes, L. E. Mechanical characterization of biodegradable implants. *Clin Mater.* **1992**, *10*, 41-46.
42. Ruedi, T. P.; Buckley, R. E.; Moran, C. G. *Principles of fracture management.* 2nd ed. Thieme: 2007.
43. Chalisgaonkar, R. Insight in applications, manufacturing and corrosion behaviour of magnesium and its alloys – A review. *Mater Today Proc.* **2020**, *26*, 1060-1071.
44. Scarritt, M. E.; Londono, R.; Badylak, S. F. Host response to implanted materials and devices: an overview. In *The immune response to implanted materials and devices: the impact of the immune system on the success of an implant*, Corradetti, B., ed. Springer International Publishing: Cham, 2017; pp 1-14.
45. Lu, Y. *Microstructure and degradation behaviour of Mg-Zn(-Ca) alloys.* University of Birmingham: Birmingham,2014.
46. Song, G.; Atrens, A. Understanding magnesium corrosion—a framework for improved alloy performance. *Adv Eng Mater.* **2003**, *5*, 837-858.
47. Ambat, R.; Aung, N. N.; Zhou, W. Studies on the influence of chloride ion and pH on the corrosion and electrochemical behaviour of AZ91D magnesium alloy. *J Appl Electrochem.* **2000**, *30*, 865-874.
48. Ambat, R.; Aung, N. N.; Zhou, W. Evaluation of microstructural effects on corrosion behaviour of AZ91D magnesium alloy. *Corros Sci.* **2000**, *42*, 1433-1455.

49. Kraus, T.; Fischerauer, S. F.; Hänzi, A. C.; Uggowitzer, P. J.; Löffler, J. F.; Weinberg, A. M. Magnesium alloys for temporary implants in osteosynthesis: in vivo studies of their degradation and interaction with bone. *Acta Biomater.* **2012**, *8*, 1230-1238.
50. Xin, Y.; Hu, T.; Chu, P. K. In vitro studies of biomedical magnesium alloys in a simulated physiological environment: a review. *Acta Biomater.* **2011**, *7*, 1452-1459.
51. Holweg, P.; Berger, L.; Cihova, M.; Donohue, N.; Clement, B.; Schwarze, U.; Sommer, N. G.; Hohenberger, G.; van den Beucken, J.; Seibert, F.; Leithner, A.; Löffler, J. F.; Weinberg, A. M. A lean magnesium-zinc-calcium alloy ZX00 used for bone fracture stabilization in a large growing-animal model. *Acta Biomater.* **2020**, *113*, 646-659.
52. Jahnen-Dechent, W.; Ketteler, M. Magnesium basics. *Clin Kidney J.* **2012**, *5*, i3-i14.
53. Shahi, A.; Aslani, S.; Ataollahi, M.; Mahmoudi, M. The role of magnesium in different inflammatory diseases. *Inflammopharmacology.* **2019**, *27*, 649-661.
54. al-Ghamdi, S. M.; Cameron, E. C.; Sutton, R. A. Magnesium deficiency: pathophysiologic and clinical overview. *Am J Kidney Dis.* **1994**, *24*, 737-752.
55. Ding, S.; Zhang, J.; Tian, Y.; Huang, B.; Yuan, Y.; Liu, C. Magnesium modification up-regulates the bioactivity of bone morphogenetic protein-2 upon calcium phosphate cement via enhanced BMP receptor recognition and Smad signaling pathway. *Colloids Surf B Biointerfaces.* **2016**, *145*, 140-151.
56. Zhou, H.; Liang, B.; Jiang, H.; Deng, Z.; Yu, K. Magnesium-based biomaterials as emerging agents for bone repair and regeneration: from mechanism to application. *J Magnes Alloys.* **2021**, *9*, 779-804.
57. Qiao, W.; Wong, K. H. M.; Shen, J.; Wang, W.; Wu, J.; Li, J.; Lin, Z.; Chen, Z.; Matinlinna, J. P.; Zheng, Y.; Wu, S.; Liu, X.; Lai, K. P.; Chen, Z.; Lam, Y. W.; Cheung, K. M. C.; Yeung, K. W. K. TRPM7 kinase-mediated immunomodulation in macrophage plays a central role in magnesium ion-induced bone regeneration. *Nat Commun.* **2021**, *12*, 2885.
58. Zhang, Y.; Xu, J.; Ruan, Y. C.; Yu, M. K.; O'Laughlin, M.; Wise, H.; Chen, D.; Tian, L.; Shi, D.; Wang, J.; Chen, S.; Feng, J. Q.; Chow, D. H.; Xie, X.; Zheng, L.; Huang, L.; Huang, S.; Leung, K.; Lu, N.; Zhao, L.; Li, H.; Zhao, D.; Guo, X.; Chan, K.; Witte, F.; Chan, H. C.; Zheng, Y.; Qin, L. Implant-derived magnesium induces local neuronal production of CGRP to improve bone-fracture healing in rats. *Nat Med.* **2016**, *22*, 1160-1169.
59. Cheng, S.; Zhang, D.; Li, M.; Liu, X.; Zhang, Y.; Qian, S.; Peng, F. Osteogenesis, angiogenesis and immune response of Mg-Al layered double hydroxide coating on pure Mg. *Bioact Mater.* **2021**, *6*, 91-105.
60. Yoshizawa, S.; Brown, A.; Barchowsky, A.; Sfeir, C. Magnesium ion stimulation of bone marrow stromal cells enhances osteogenic activity, simulating the effect of magnesium alloy degradation. *Acta Biomater.* **2014**, *10*, 2834-2842.
61. Salimi, M. H.; Heughebaert, J. C.; Nancollas, G. H. Crystal growth of calcium phosphates in the presence of magnesium ions. *Langmuir.* **1985**, *1*, 119-122.
62. Fox, C.; Ramsoomair, D.; Carter, C. Magnesium: its proven and potential clinical significance. *South Med J.* **2001**, *94*, 1195-1201.
63. Musso, C. G. Magnesium metabolism in health and disease. *Int Urol Nephrol.* **2009**, *41*, 357-362.
64. Institute of Medicine Standing Committee on the Scientific Evaluation of Dietary Reference, I. The National Academies Collection: Reports funded by National Institutes of Health. In Dietary Reference Intakes for Calcium, Phosphorus, Magnesium, Vitamin D, and Fluoride, National Academies Press (US): Washington (DC), 1997.
65. Office of Dietary Supplements, National Institutes of Health. Magnesium: fact sheet for health professionals. https://ods.od.nih.gov/factsheets/Magnesium-HealthProfessional/. Accessed May 1, 2021.
66. Windhagen, H.; Radtke, K.; Weizbauer, A.; Diekmann, J.; Noll, Y.; Kreimeyer, U.; Schavan, R.; Stukenborg-Colsman, C.; Waizy, H. Biodegradable magnesium-based screw clinically equivalent to titanium screw in hallux valgus surgery: short term results of the first prospective, randomized, controlled clinical pilot study. *Biomed Eng Online.* **2013**, *12*, 62.
67. Willbold, E.; Kaya, A. A.; Kaya, R. A.; Beckmann, F.; Witte, F. Corrosion of magnesium alloy AZ31 screws is dependent on the implantation site. *Mater Sci Eng B.* **2011**, *176*, 1835-1840.
68. Thomann, M.; Krause, C.; Bormann, D.; von der Höh, N.; Windhagen, H.; Meyer-Lindenberg, A. Comparison of the resorbable magnesium . alloys LAE442 und MgCa0.8 concerning their mechanical properties, their progress of degradation and the bone-implant-contact after 12 months implantation duration in a rabbit model. *Materialwiss Werkstofftech.* **2009**, *40*, 82-87.
69. Gilbert, S. G. *A small dose of toxicology: the health effects of common chemicals.* CRC Press: 2004.
70. World Health Organization, International Atomic Energy Agency & Food and Agriculture Organization of the United Nations. *Trace elements in human nutrition and health.* World Health Organization: Geneva, 1996.
71. Alzheimer's Society. Aluminium, metals and dementia. https://www.alzheimers.org.uk/about-dementia/risk-factors-and-prevention/metals-and-dementia. Accessed May 1, 2021.
72. Exley, C. The coordination chemistry of aluminium in neurodegenerative disease. *Coord Chem Rev.* **2012,** *256*, 2142-2146.
73. Exley, C. What is the risk of aluminium as a neurotoxin? *Expert Rev Neurother.* **2014**, *14*, 589-591.
74. Liu, X.; Shan, D.; Song, Y.; Han, E.H. Influence of yttrium element on the corrosion behaviors of Mg–Y binary magnesium alloy. *J Magnes Alloys.* **2017**, *5*, 26-34.
75. Miller, P. L.; Shaw, B. A.; Wendt, R. G.; Moshier, W. C. Assessing the corrosion resistance of nonequilibrium magnesium-yttrium alloys. *Corrosion.* **1995**, *51*, 922-931.
76. McCarty, M. F. Reported antiatherosclerotic activity of silicon may reflect increased endothelial synthesis of heparan sulfate proteoglycans. *Med Hypotheses.* **1997**, *49*, 175-176.
77. Pors Nielsen, S. The biological role of strontium. *Bone.* **2004**, *35*, 583-588.
78. Avedesian, M.; Baker, H. *ASM specialty handbook: magnesium and magnesium alloys.* ASM International: 1999.
79. Aa, N.; Clark, J. Phase diagram of binary magnesium alloys. ASM International Monograph Series on Alloy Phase Diagrams. 1988.
80. Purcell, F. K.; Kotz, C. J. 4.3: Electrochemical potentials. https://chem.libretexts.org/Bookshelves/Inorganic_Chemistry/Book%3A_Introduction_to_Inorganic_Chemistry/04%3A_Redox_Stability_and_Redox_Reactions/4.03%3A_Electrochemical_Potentials. Accessed June 4, 2021.
81. CrystalMaker Software Ltd. Elements, atomic radii and the periodic table: How big is an atom? Why does its size vary? How can we show this in CrystalMaker? http://crystalmaker.com/support/tutorials/atomic-radii/index.html. Accessed May 2, 2021.

82. Witte, F.; Hort, N.; Vogt, C.; Cohen, S.; Kainer, K. U.; Willumeit, R.; Feyerabend, F. Degradable biomaterials based on magnesium corrosion. *Curr Opin Solid State Mater Sci.* **2008**, *12*, 63-72.
83. Kirkland, N. T.; Staiger, M. P.; Nisbet, D.; Davies, C. H. J.; Birbilis, N. Performance-driven design of Biocompatible Mg alloys. *JOM.* **2011**, *63*, 28-34.
84. Chen, Y.; Xu, Z.; Smith, C.; Sankar, J. Recent advances on the development of magnesium alloys for biodegradable implants. *Acta Biomater.* **2014**, *10*, 4561-4573.
85. Lenntech. Recommended daily intake of vitamins and minerals. https://www.lenntech.com/recommended-daily-intake.htm. Accessed May 2, 2021.
86. Easton, M. A.; StJohn, D. H. A model of grain refinement incorporating alloy constitution and potency of heterogeneous nucleant particles. *Acta Mater.* **2001**, *49*, 1867-1878.
87. Easton, M.; StJohn, D. Grain refinement of aluminum alloys: Part I. the nucleant and solute paradigms—a review of the literature. *Metall Mater Trans A.* **1999**, *30*, 1613-1623.
88. Easton, M.; StJohn, D. Grain refinement of aluminum alloys: Part II. Confirmation of, and a mechanism for, the solute paradigm. *Metall Mater Trans A.* **1999**, *30*, 1625-1633.
89. StJohn, D. H.; Qian, M.; Easton, M. A.; Cao, P.; Hildebrand, Z. Grain refinement of magnesium alloys. *Metall Mater Trans A.* **2005**, *36*, 1669-1679.
90. Lee, Y. C.; Dahle, A. K.; StJohn, D. H. The role of solute in grain refinement of magnesium. Metall Mater Trans A. 2000, 31, 2895-2906.
91. Song, G. L.; Atrens, A. Corrosion mechanisms of magnesium alloys. *Adv Eng Mater.* **1999**, *1*, 11-33.
92. Velikokhatnyi, O. I.; Kumta, P. N. First-principles studies on alloying and simplified thermodynamic aqueous chemical stability of calcium-, zinc-, aluminum-, yttrium- and iron-doped magnesium alloys. *Acta Biomater.* **2010**, *6*, 1698-1704.
93. Li, H.; Wang, P.; Lin, G.; Huang, J. The role of rare earth elements in biodegradable metals: A review. *Acta Biomater.* **2021**, *129*, 33-42.
94. Zhang, X.; Yuan, G.; Mao, L.; Niu, J.; Ding, W. Biocorrosion properties of as-extruded Mg–Nd–Zn–Zr alloy compared with commercial AZ31 and WE43 alloys. *Mater Lett.* **2012**, *66*, 209-211.
95. Wang, L.; Li, J. B.; Li, L.; Nie, K. B.; Zhang, J. S.; Yang, C. W.; Yan, P. W.; Liu, Y. P.; Xu, C. X. Microstructure, mechanical and bio-corrosion properties of Mg–Zn–Zr alloys with minor Ca addition. *Mater Sci Technol.* **2017**, *33*, 9-16.
96. Yin, D. S.; Zhang, E. L.; Zeng, S. Y. Effect of Zn on mechanical property and corrosion property of extruded Mg-Zn-Mn alloy. *Trans Nonferrous Metals Soc China.* **2008**, *18*, 763-768.
97. Kang, Y. H.; Wu, D.; Chen, R. S.; Han, E. H. Microstructures and mechanical properties of the age hardened Mg–4.2Y–2.5Nd–1Gd–0.6Zr (WE43) microalloyed with Zn. *J Magnes Alloys.* **2014**, *2*, 109-115.
98. Hänzi, A. C.; Gerber, I.; Schinhammer, M.; Löffler, J. F.; Uggowitzer, P. J. On the in vitro and in vivo degradation performance and biological response of new biodegradable Mg-Y-Zn alloys. *Acta Biomater.* **2010**, *6*, 1824-1833.
99. Peng, Q.; Huang, Y.; Zhou, L.; Hort, N.; Kainer, K. U. Preparation and properties of high purity Mg-Y biomaterials. *Biomaterials.* **2010**, *31*, 398-403.
100. Lu, Y.; Bradshaw, A. R.; Chiu, Y. L.; Jones, I. P. The role of β1' precipitates in the bio-corrosion performance of Mg–3Zn in simulated body fluid. *J Alloys Compd.* **2014**, *614*, 345-352.
101. Cheng, M.; Chen, J.; Yan, H.; Su, B.; Yu, Z.; Xia, W.; Gong, X. Effects of minor Sr addition on microstructure, mechanical and bio-corrosion properties of the Mg-5Zn based alloy system. *J Alloys Compd.* **2017**, *691*, 95-102.
102. Lu, Y.; Chiu, Y. L.; Jones, I. P. Three-dimensional analysis of the microstructure and bio-corrosion of Mg–Zn and Mg–Zn–Ca alloys. *Mater Charact.* **2016**, *112*, 113-121.
103. Li, Z.; Gu, X.; Lou, S.; Zheng, Y. The development of binary Mg-Ca alloys for use as biodegradable materials within bone. *Biomaterials.* **2008**, *29*, 1329-1344.
104. Sun, Y.; Zhang, B.; Wang, Y.; Geng, L.; Jiao, X. Preparation and characterization of a new biomedical Mg–Zn–Ca alloy. *Mater Des.* **2012**, *34*, 58-64.
105. Lu, Y.; Ding, R. G.; Chiu, Y. L.; Jones, I. P. Tomographic investigation of the effects of second phases on the biodegradation and nano-mechanical performance of a Mg–Zn–Ca alloy. *Materialia.* **2018**, *4*, 1-9.
106. Zhang, E.; Yang, L.; Xu, J.; Chen, H. Microstructure, mechanical properties and bio-corrosion properties of Mg-Si(-Ca, Zn) alloy for biomedical application. *Acta Biomater.* **2010**, *6*, 1756-1762.
107. Zhao, C.; Pan, F.; Zhang, L.; Pan, H.; Song, K.; Tang, A. Microstructure, mechanical properties, bio-corrosion properties and cytotoxicity of as-extruded Mg-Sr alloys. *Mater Sci Eng C Mater Biol Appl.* **2017**, *70*, 1081-1088.
108. Wen, Z.; Wu, C.; Dai, C.; Yang, F. Corrosion behaviors of Mg and its alloys with different Al contents in a modified simulated body fluid. *J Alloys Compd.* **2009**, *488*, 392-399.
109. Witte, F.; Fischer, J.; Nellesen, J.; Crostack, H. A.; Kaese, V.; Pisch, A.; Beckmann, F.; Windhagen, H. In vitro and in vivo corrosion measurements of magnesium alloys. *Biomaterials.* **2006**, *27*, 1013-1018.
110. Zhang, B.; Hou, Y.; Wang, X.; Wang, Y.; Geng, L. Mechanical properties, degradation performance and cytotoxicity of Mg–Zn–Ca biomedical alloys with different compositions. *Mater Sci Eng C.* **2011**, *31*, 1667-1673.
111. Lu, Y.; Bradshaw, A. R.; Chiu, Y. L.; Jones, I. P. Effects of secondary phase and grain size on the corrosion of biodegradable Mg-Zn-Ca alloys. *Mater Sci Eng C Mater Biol Appl.* **2015**, *48*, 480-486.
112. Cho, D. H.; Lee, B. W.; Park, J. Y.; Cho, K. M.; Park, I. M. Effect of Mn addition on corrosion properties of biodegradable Mg-4Zn-0.5Ca-xMn alloys. *J Alloys Compd.* **2017**, *695*, 1166-1174.
113. Zhang, E.; He, W.; Du, H.; Yang, K. Microstructure, mechanical properties and corrosion properties of Mg–Zn–Y alloys with low Zn content. *Mater Sci Eng A.* **2008**, *488*, 102-111.
114. Zhang, X.; Wu, Y.; Xue, Y.; Wang, Z.; Yang, L. Biocorrosion behavior and cytotoxicity of a Mg–Gd–Zn–Zr alloy with long period stacking ordered structure. *Mater Lett.* **2012**, *86*, 42-45.
115. Krause, A.; von der Höh, N.; Bormann, D.; Krause, C.; Bach, F. W.; Windhagen, H.; Meyer-Lindenberg, A. Degradation behaviour and mechanical properties of magnesium implants in rabbit tibiae. *J Mater Sci.* **2010**, *45*, 624-632.
116. Gu, X. N.; Xie, X. H.; Li, N.; Zheng, Y. F.; Qin, L. In vitro and in vivo studies on a Mg-Sr binary alloy system developed as a new kind of biodegradable metal. *Acta Biomater.* **2012**, *8*, 2360-2374.
117. Zhang, S.; Zhang, X.; Zhao, C.; Li, J.; Song, Y.; Xie, C.; Tao, H.; Zhang, Y.; He, Y.; Jiang, Y.; Bian, Y. Research on an Mg-Zn alloy as a degradable biomaterial. *Acta Biomater.* **2010**, *6*, 626-640.
118. Li, N.; Zheng, Y. Novel magnesium alloys developed for biomedical application: a review. *J Mater Sci Technol.* **2013**, *29*, 489-502.
119. Song, G.; Atrens, A.; Dargusch, M. Influence of microstructure on the corrosion of diecast AZ91D. *Corros Sci.* **1998**, *41*, 249-273.

120. Aung, N. N.; Zhou, W. Effect of grain size and twins on corrosion behaviour of AZ31B magnesium alloy. *Corros Sci.* **2010**, *52*, 589-594.
121. Hamu, G. B.; Eliezer, D.; Wagner, L. The relation between severe plastic deformation microstructure and corrosion behavior of AZ31 magnesium alloy. *J Alloys Compd.* **2009**, *468*, 222-229.
122. Birbilis, N.; Ralston, K. D.; Virtanen, S.; Fraser, H. L.; Davies, C. H. J. Grain character influences on corrosion of ECAPed pure magnesium. *Corros Eng Sci Technol.* **2010**, *45*, 224-230.
123. Ralston, K. D.; Birbilis, N.; Davies, C. H. J. Revealing the relationship between grain size and corrosion rate of metals. *Scripta Mater.* **2010**, *63*, 1201-1204.
124. op't Hoog, C.; Birbilis, N.; Estrin, Y. Corrosion of pure Mg as a function of grain size and processing route. *Adv Eng Mater.* **2008**, *10*, 579-582.
125. Jang, Y. H.; Kim, S. S.; Yim, C. D.; Lee, C. G.; Kim, S. J. Corrosion behaviour of friction stir welded AZ31B Mg in 3•5%NaCl solution. *Corros Eng Sci Technol.* **2007**, *42*, 119-122.
126. Song, G.; StJohn, D. The effect of zirconium grain refinement on the corrosion behaviour of magnesium-rare earth alloy MEZ. *J Light Metals.* **2002**, *2*, 1-16.
127. Song, G. Recent progress in corrosion and protection of magnesium alloys. *Adv Eng Mater.* **2005**, *7*, 563-586.
128. Lunder, O.; Lein, J. E.; Aune, T. K.; Nisancioglu, K. The role of $Mg_{17}Al_{12}$ phase in the corrosion of Mg alloy AZ91. *Corrosion.* **1989**, *45*, 741-748.
129. Beldjoudi, T.; Fiaud, C.; Robbiola, L. Influence of homogenization and artificial aging heat treatments on corrosion behavior of Mg-Al alloys. *Corrosion.* **1993**, *49*, 738-745.
130. Pardo, A.; Merino, M. C.; Coy, A. E.; Arrabal, R.; Viejo, F.; Matykina, E. Corrosion behaviour of magnesium/aluminium alloys in 3.5wt.% NaCl. *Corros Sci.* **2008**, *50*, 823-834.
131. Lunder, O.; Videm, M.; Nisancioglu, K. Corrosion resistant magnesium alloys. *SAE Trans.* **1995**, *104*, 352-357.
132. Srinivasan, A.; Ningshen, S.; Kamachi Mudali, U.; Pillai, U. T. S.; Pai, B. C. Influence of Si and Sb additions on the corrosion behavior of AZ91 magnesium alloy. *Intermetallics.* **2007**, *15*, 1511-1517.
133. Mao, L.; Shen, L.; Chen, J.; Zhang, X.; Kwak, M.; Wu, Y.; Fan, R.; Zhang, L.; Pei, J.; Yuan, G.; Song, C.; Ge, J.; Ding, W. A promising biodegradable magnesium alloy suitable for clinical vascular stent application. *Sci Rep.* **2017**, *7*, 46343.
134. Zhang, X.; Yuan, G.; Mao, L.; Niu, J.; Fu, P.; Ding, W. Effects of extrusion and heat treatment on the mechanical properties and biocorrosion behaviors of a Mg-Nd-Zn-Zr alloy. *J Mech Behav Biomed Mater.* **2012**, *7*, 77-86.
135. Zong, Y.; Yuan, G.; Zhang, X.; Mao, L.; Niu, J.; Ding, W. Comparison of biodegradable behaviors of AZ31 and Mg–Nd–Zn–Zr alloys in Hank's physiological solution. *Mater Sci Eng B.* **2012**, *177*, 395-401.
136. Andrei, M.; Eliezer, A.; Bonora, P. L.; Gutman, E. M. DC and AC polarisation study on magnesium alloys Influence of the mechanical deformation. *Mater Corros.* **2002**, *53*, 455-461.
137. Xin, R. L.; Wang, M. Y.; Gao, J. C.; Liu, P.; Liu, Q. Effect of microstructure and texture on corrosion resistance of magnesium alloy. *Mater Sci Forum.* **2009**, *610-613*, 1160-1163.
138. Schmutz, P.; Guillaumin, V.; Lillard, R. S.; Lillard, J. A.; Frankel, G. S. Influence of dichromate ions on corrosion processes on pure magnesium. *J Electrochem Soc.* **2003**, *150*, B99.
139. Gu, X.; Zheng, Y.; Zhong, S.; Xi, T.; Wang, J.; Wang, W. Corrosion of, and cellular responses to Mg-Zn-Ca bulk metallic glasses. *Biomaterials.* **2010**, *31*, 1093-1103.
140. Zberg, B.; Uggowitzer, P. J.; Löffler, J. F. MgZnCa glasses without clinically observable hydrogen evolution for biodegradable implants. *Nat Mater.* **2009**, *8*, 887-891.
141. Zhang, X. L.; Chen, G.; Bauer, T. Mg-based bulk metallic glass composite with high bio-corrosion resistance and excellent mechanical properties. *Intermetallics.* **2012**, *29*, 56-60.
142. Zberg, B.; Arata, E. R.; Uggowitzer, P. J.; Löffler, J. F. Tensile properties of glassy MgZnCa wires and reliability analysis using Weibull statistics. *Acta Mater.* **2009**, *57*, 3223-3231.
143. Park, E. S.; Kim, W. T.; Kim, D. H. Bulk glass formation in Mg-Cu-Ag-Y-Gd alloy. *Mater Trans.* **2004**, *45*, 2474-2477.
144. Sun, Y.; Zhang, H. F.; Fu, H. M.; Wang, A. M.; Hu, Z. Q. Mg–Cu–Ag–Er bulk metallic glasses with high glass forming ability and compressive strength. *Mater Sci Eng A.* **2009**, *502*, 148-152.
145. Wessels, V.; Le Mené, G.; Fischerauer, S. F.; Kraus, T.; Weinberg, A. M.; Uggowitzer, P. J.; Löffler, J. F. In vivo performance and structural relaxation of biodegradable bone implants made from Mg Zn Ca bulk metallic glasses. *Adv Eng Mater.* **2012**, *14*, B357-B364.
146. Yu, H. J.; Wang, J. Q.; Shi, X. T.; Louzguine-Luzgin, D. V.; Wu, H.-K.; Perepezko, J. H. Ductile biodegradable Mg-based metallic glasses with excellent biocompatibility. *Adv Funct Mater.* **2013**, *23*, 4793-4800.
147. Ashby, M. F.; Greer, A. L. Metallic glasses as structural materials. *Scripta Mater.* **2006**, *54*, 321-326.
148. Razavi, M.; Fathi, M. H.; Meratian, M. Microstructure, mechanical properties and bio-corrosion evaluation of biodegradable AZ91-FA nanocomposites for biomedical applications. *Mater Sci Eng A.* **2010**, *527*, 6938-6944.
149. Lei, T.; Tang, W.; Cai, S. H.; Feng, F. F.; Li, N. F. On the corrosion behaviour of newly developed biodegradable Mg-based metal matrix composites produced by in situ reaction. *Corros Sci.* **2012**, *54*, 270-277.
150. Feng, A.; Han, Y. The microstructure, mechanical and corrosion properties of calcium polyphosphate reinforced ZK60A magnesium alloy composites. *J Alloys Compd.* **2010**, *504*, 585-593.
151. Gu, X.; Zhou, W.; Zheng, Y.; Dong, L.; Xi, Y.; Chai, D. Microstructure, mechanical property, bio-corrosion and cytotoxicity evaluations of Mg/HA composites. *Mater Sci Eng C.* **2010**, *30*, 827-832.
152. Ye, X.; Chen, M.; Yang, M.; Wei, J.; Liu, D. In vitro corrosion resistance and cytocompatibility of nano-hydroxyapatite reinforced Mg–Zn–Zr composites. *J Mater Sci Mater Med.* **2010**, *21*, 1321-1328.
153. Liu, D.; Zuo, Y.; Meng, W.; Chen, M.; Fan, Z. Fabrication of biodegradable nano-sized β-TCP/Mg composite by a novel melt shearing technology. *Mater Sci Eng C.* **2012**, *32*, 1253-1258.
154. Wang, T.; Lin, C.; Batalu, D.; Zhang, L.; Hu, J.; Lu, W. In vitro study of the PLLA-Mg65Zn30Ca5 composites as potential biodegradable materials for bone implants. *J Magnes Alloys.* ***2021***. doi:10.1016/j.jma.2020.12.014.
155. Antoniac, I. V.; Antoniac, A.; Vasile, E.; Tecu, C.; Fosca, M.; Yankova, V. G.; Rau, J. V. In vitro characterization of novel nanostructured collagen-hydroxyapatite composite scaffolds doped with magnesium with improved biodegradation rate for hard tissue regeneration. *Bioact Mater.* **2021**, *6*, 3383-3395.
156. Shen, J.; Chen, B.; Zhai, X.; Qiao, W.; Wu, S.; Liu, X.; Zhao, Y.; Ruan, C.; Pan, H.; Chu, P. K.; Cheung, K. M. C.; Yeung, K. W. K. Stepwise 3D-spatio-temporal magnesium cationic niche: Nanocomposite scaffold mediated microenvironment for modulating intramembranous ossification. *Bioact Mater.* **2021**, *6*, 503-519.
157. Shen, J.; Wang, W.; Zhai, X.; Chen, B.; Qiao, W.; Li, W.; Li, P.; Zhao, Y.; Meng, Y.; Qian, S.; Liu, X.; Chu, P. K.; Yeung, K. W. K.

3D-printed nanocomposite scaffolds with tunable magnesium ionic microenvironment induce in situ bone tissue regeneration. *Appl Mater Today*. **2019**, *16*, 493-507.
158. Wang, X.; Xu, S.; Zhou, S.; Xu, W.; Leary, M.; Choong, P.; Qian, M.; Brandt, M.; Xie, Y. M. Topological design and additive manufacturing of porous metals for bone scaffolds and orthopaedic implants: A review. *Biomaterials*. **2016**, *83*, 127-141.
159. Zou, X.; Li, H.; Bünger, M.; Egund, N.; Lind, M.; Bünger, C. Bone ingrowth characteristics of porous tantalum and carbon fiber interbody devices: an experimental study in pigs. *Spine J*. **2004**, *4*, 99-105.
160. Pamula, E.; Bacakova, L.; Filova, E.; Buczynska, J.; Dobrzynski, P.; Noskova, L.; Grausova, L. The influence of pore size on colonization of poly(L-lactide-glycolide) scaffolds with human osteoblast-like MG 63 cells in vitro. *J Mater Sci Mater Med*. **2008**, *19*, 425-435.
161. Pamula, E.; Filová, E.; Bacáková, L.; Lisá, V.; Adamczyk, D. Resorbable polymeric scaffolds for bone tissue engineering: the influence of their microstructure on the growth of human osteoblast-like MG 63 cells. *J Biomed Mater Res A*. **2009**, *89*, 432-443.
162. Lefebvre, L. P.; Banhart, J.; Dunand, D. C. Porous metals and metallic foams: current status and recent developments. *Adv Eng Mater*. **2008**, *10*, 775-787.
163. Cheng, M. Q.; Wahafu, T.; Jiang, G. F.; Liu, W.; Qiao, Y. Q.; Peng, X. C.; Cheng, T.; Zhang, X. L.; He, G.; Liu, X. Y. A novel open-porous magnesium scaffold with controllable microstructures and properties for bone regeneration. *Sci Rep*. **2016**, *6*, 24134.
164. Razavi, M.; Fathi, M.; Savabi, O.; Vashaee, D.; Tayebi, L. In vitro study of nanostructured diopside coating on Mg alloy orthopedic implants. *Mater Sci Eng C Mater Biol Appl*. **2014**, *41*, 168-177.
165. Li, Y.; Zhou, J.; Pavanram, P.; Leeflang, M. A.; Fockaert, L. I.; Pouran, B.; Tümer, N.; Schröder, K. U.; Mol, J. M. C.; Weinans, H.; Jahr, H.; Zadpoor, A. A. Additively manufactured biodegradable porous magnesium. *Acta Biomater*. **2018**, *67*, 378-392.
166. Geng, F.; Tan, L.; Zhang, B.; Wu, C.; He, Y.; Yang, J.; Yang, K. Study on β-TCP coated porous Mg as a bone tissue engineering scaffold material. *J Mater Sci Technol*. **2009**, *25*, 123-129.
167. Tan, L.; Gong, M.; Zheng, F.; Zhang, B.; Yang, K. Study on compression behavior of porous magnesium used as bone tissue engineering scaffolds. *Biomed Mater*. **2009**, *4*, 015016.
168. Witte, F.; Ulrich, H.; Palm, C.; Willbold, E. Biodegradable magnesium scaffolds: Part II: peri-implant bone remodeling. *J Biomed Mater Res A*. **2007**, *81*, 757-765.
169. Gu, X. N.; Zhou, W. R.; Zheng, Y. F.; Liu, Y.; Li, Y. X. Degradation and cytotoxicity of lotus-type porous pure magnesium as potential tissue engineering scaffold material. *Mater Lett*. **2010**, *64*, 1871-1874.
170. Badekila, A. K.; Kini, S.; Jaiswal, A. K. Fabrication techniques of biomimetic scaffolds in three-dimensional cell culture: A review. *J Cell Physiol*. **2021**, *236*, 741-762.
171. Zhao, D.; Witte, F.; Lu, F.; Wang, J.; Li, J.; Qin, L. Current status on clinical applications of magnesium-based orthopaedic implants: A review from clinical translational perspective. *Biomaterials*. **2017**, *112*, 287-302.
172. ASTM B557. Standard test methods for tension testing wrought and castaluminum- and magnesium-alloy products. 2015.
173. International Organization of Standards. ISO 6892-1:Metallic materials-Tensile testing-Part1: Method of test at room temperature. 2019.
174. ASTM WK61103. New guide for corrosion fatigueevaluation of absorbablemetals. 2017.
175. Jalota, S.; Bhaduri, S. B.; Tas, A. C. Using a synthetic body fluid (SBF) solution of 27 mM HCO_3^- to make bone substitutes more osteointegrative. *Mater Sci Eng C*. **2008**, *28*, 129-140.
176. Zhang, X.; Yuan, G.; Niu, J.; Fu, P.; Ding, W. Microstructure, mechanical properties, biocorrosion behavior, and cytotoxicity of as-extruded Mg-Nd-Zn-Zr alloy with different extrusion ratios. *J Mech Behav Biomed Mater*. **2012**, *9*, 153-162.
177. Wang, H.; Estrin, Y.; Fu, H.; Song, G.; Zúberová, Z. The Effect of pre-processing and grain structure on the bio-corrosion and fatigue resistance of magnesium alloy AZ31. *Adv Eng Mater*. **2007**, *9*, 967-972.
178. Witte, F.; Feyerabend, F.; Maier, P.; Fischer, J.; Störmer, M.; Blawert, C.; Dietzel, W.; Hort, N. Biodegradable magnesium-hydroxyapatite metal matrix composites. *Biomaterials*. **2007**, *28*, 2163-2174.
179. Wang, Y.; Wei, M.; Gao, J. Improve corrosion resistance of magnesium in simulated body fluid by dicalcium phosphate dihydrate coating. *Mater Sci Eng C*. **2009**, *29*, 1311-1316.
180. Kirkland, N. T.; Lespagnol, J.; Birbilis, N.; Staiger, M. P. A survey of bio-corrosion rates of magnesium alloys. *Corros Sci*. **2010**, *52*, 287-291.
181. Hort, N.; Huang, Y.; Fechner, D.; Störmer, M.; Blawert, C.; Witte, F.; Vogt, C.; Drücker, H.; Willumeit, R.; Kainer, K. U.; Feyerabend, F. Magnesium alloys as implant materials--principles of property design for Mg-RE alloys. *Acta Biomater*. **2010**, *6*, 1714-1725.
182. Song, G. L.; Atrens, A.; St.John, D. H. *Magnesium technology*. New Orleans,**2001**.
183. Alvarez-Lopez, M.; Pereda, M. D.; del Valle, J. A.; Fernandez-Lorenzo, M.; Garcia-Alonso, M. C.; Ruano, O. A.; Escudero, M. L. Corrosion behaviour of AZ31 magnesium alloy with different grain sizes in simulated biological fluids. *Acta Biomater*. **2010**, *6*, 1763-1771.
184. He, W.; Zhang, E.; Yang, K. Effect of Y on the bio-corrosion behavior of extruded Mg–Zn–Mn alloy in Hank's solution. *Mater Sci Eng C*. **2010**, *30*, 167-174.
185. Kannan, M. B. Influence of microstructure on the in-vitro degradation behaviour of magnesium alloys. *Mater Lett*. **2010**, *64*, 739-742.
186. Kirkland, N. T.; Birbilis, N.; Staiger, M. P. Assessing the corrosion of biodegradable magnesium implants: a critical review of current methodologies and their limitations. *Acta Biomater*. **2012**, *8*, 925-936.
187. Song, G.; Atrens, A.; Wu, X.; Zhang, B. Corrosion behaviour of AZ21, AZ501 and AZ91 in sodium chloride. *Corros Sci*. **1998**, *40*, 1769-1791.
188. Parai, R.; Bandyopadhyay-Ghosh, S. Engineered bio-nanocomposite magnesium scaffold for bone tissue regeneration. *J Mech Behav Biomed Mater*. **2019**, *96*, 45-52.
189. Dutta, S.; Devi, K. B.; Gupta, S.; Kundu, B.; Balla, V. K.; Roy, M. Mechanical and in vitro degradation behavior of magnesium-bioactive glass composites prepared by SPS for biomedical applications. *J Biomed Mater Res B Appl Biomater*. **2019**, *107*, 352-365.
190. Chen, K.; Xie, X.; Tang, H.; Sun, H.; Qin, L.; Zheng, Y.; Gu, X.; Fan, Y. In vitro and in vivo degradation behavior of Mg-2Sr-Ca and Mg-2Sr-Zn alloys. *Bioact Mater*. **2020**, *5*, 275-285.
191. Heublein, B.; Rohde, R.; Kaese, V.; Niemeyer, M.; Hartung, W.; Haverich, A. Biocorrosion of magnesium alloys: a new principle in cardiovascular implant technology? *Heart*. **2003**, *89*, 651-656.
192. Kaya, R. A.; Cavuşoğlu, H.; Tanik, C.; Kaya, A. A.; Duygulu, O.; Mutlu, Z.; Zengin, E.; Aydin, Y. The effects of magnesium particles in posterolateral spinal fusion: an experimental in vivo study in a sheep model. *J Neurosurg Spine*. **2007**, *6*, 141-149.
193. Huang, S.; Wang, B.; Zhang, X.; Lu, F.; Wang, Z.; Tian, S.; Li, D.; Yang, J.; Cao, F.; Cheng, L.; Gao, Z.; Li, Y.; Qin, K.; Zhao, D. High-purity weight-bearing magnesium screw: Translational application in

the healing of femoral neck fracture. *Biomaterials.* **2020**, *238*, 119829.
194. Grün, N. G.; Holweg, P.; Tangl, S.; Eichler, J.; Berger, L.; van den Beucken, J.; Löffler, J. F.; Klestil, T.; Weinberg, A. M. Comparison of a resorbable magnesium implant in small and large growing-animal models. *Acta Biomater.* **2018**, *78*, 378-386.
195. Huang, Q.; Liu, L.; Wu, H.; Li, K.; Li, N.; Liu, Y. The design, development, and in vivo performance of intestinal anastomosis ring fabricated by magnesium-zinc-strontium alloy. *Mater Sci Eng C Mater Biol Appl.* **2020**, *106*, 110158.
196. Imwinkelried, T.; Beck, S.; Schaller, B. Pre-clinical testing of human size magnesium implants in miniature pigs: Implant degradation and bone fracture healing at multiple implantation sites. *Mater Sci Eng C Mater Biol Appl.* **2020**, *108*, 110389.
197. Li, W.; Zhou, J.; Xu, Y. Study of the in vitro cytotoxicity testing of medical devices. *Biomed Rep.* **2015**, *3*, 617-620.
198. International Organization of Standards. ISO 10993-5: biological evaluation of medical devices: tests for in vitro cytotoxicity.
199. De Melo, W. M.; Maximiano, W. M.; Antunes, A. A.; Beloti, M. M.; Rosa, A. L.; de Oliveira, P. T. Cytotoxicity testing of methyl and ethyl 2-cyanoacrylate using direct contact assay on osteoblast cell cultures. *J Oral Maxillofac Surg.* **2013**, *71*, 35-41.
200. Sjögren, G.; Sletten, G.; Dahl, J. E. Cytotoxicity of dental alloys, metals, and ceramics assessed by millipore filter, agar overlay, and MTT tests. *J Prosthet Dent.* **2000**, *84*, 229-236.
201. Jin, C. Y.; Zhu, B. S.; Wang, X. F.; Lu, Q. H. Cytotoxicity of titanium dioxide nanoparticles in mouse fibroblast cells. *Chem Res Toxicol.* **2008**, *21*, 1871-1877.
202. Liu, L.; Huang, B.; Liu, X.; Yuan, W.; Zheng, Y.; Li, Z.; Yeung, K. W. K.; Zhu, S.; Liang, Y.; Cui, Z.; Wu, S. Photo-controlled degradation of PLGA/Ti(3)C(2) hybrid coating on Mg-Sr alloy using near infrared light. *Bioact Mater.* **2021**, *6*, 568-578.
203. Han, D.; Li, Y.; Liu, X.; Yeung, K. W. K.; Zheng, Y.; Cui, Z.; Liang, Y.; Li, Z.; Zhu, S.; Wang, X.; Wu, S. Photothermy-strengthened photocatalytic activity of polydopamine-modified metal-organic frameworks for rapid therapy of bacteria-infected wounds. *J Mater Sci Technol.* **2021**, *62*, 83-95.
204. Sarkar, K.; Rahaman, M.; Agarwal, S.; Bodhak, S.; Halder, S.; Nandi, S. K.; Roy, M. Degradability and in vivo biocompatibility of doped magnesium phosphate bioceramic scaffolds. *Mater Lett.* **2020**, *259*, 126892.
205. Kumar, V.; Sarkar, K.; Bavya Devi, K.; Ghosh, D.; Nandi, S. K.; Roy, M. Quantitative assessment of degradation, cytocompatibility, and in vivo bone regeneration of silicon-incorporated magnesium phosphate bioceramics. *J Mater Res.* **2019**, *34*, 4024-4036.
206. Wang, J.; Cui, L.; Ren, Y.; Zou, Y.; Ma, J.; Wang, C.; Zheng, Z.; Chen, X.; Zeng, R.; Zheng, Y. In vitro and in vivo biodegradation and biocompatibility of an MMT/BSA composite coating upon magnesium alloy AZ31. *J Mater Sci Technol.* **2020**, *47*, 52-67.
207. Lin, Z.; Zhao, Y.; Chu, P. K.; Wang, L.; Pan, H.; Zheng, Y.; Wu, S.; Liu, X.; Cheung, K. M. C.; Wong, T.; Yeung, K. W. K. A functionalized TiO(2)/Mg(2)TiO(4) nano-layer on biodegradable magnesium implant enables superior bone-implant integration and bacterial disinfection. *Biomaterials.* **2019**, *219*, 119372.
208. Makkar, P.; Kang, H. J.; Padalhin, A. R.; Faruq, O.; Lee, B. In-vitro and in-vivo evaluation of strontium doped calcium phosphate coatings on biodegradable magnesium alloy for bone applications. *Appl Surf Sci.* **2020**, *510*, 145333.
209. International Organization of Standards. ISO 10993-12: biological evaluation of medical devices: sample preparation and reference materials.
210. Yamamoto, A.; Hiromoto, S. Effect of inorganic salts, amino acids and proteins on the degradation of pure magnesium in vitro. *Mater Sci Eng C.* **2009**, *29*, 1559-1568.
211. Fischer, J.; Pröfrock, D.; Hort, N.; Willumeit, R.; Feyerabend, F. Improved cytotoxicity testing of magnesium materials. *Mater Sci Eng B.* **2011**, *176*, 830-834.
212. Wang, J.; Witte, F.; Xi, T.; Zheng, Y.; Yang, K.; Yang, Y.; Zhao, D.; Meng, J.; Li, Y.; Li, W.; Chan, K.; Qin, L. Recommendation for modifying current cytotoxicity testing standards for biodegradable magnesium-based materials. *Acta Biomater.* **2015**, *21*, 237-249.
213. Jablonská, E.; Kubásek, J.; Vojtěch, D.; Ruml, T.; Lipov, J. Test conditions can significantly affect the results of in vitro cytotoxicity testing of degradable metallic biomaterials. *Sci Rep.* **2021**, *11*, 6628.
214. Razavi, M.; Fathi, M.; Savabi, O.; Razavi, S. M.; Heidari, F.; Manshaei, M.; Vashaee, D.; Tayebi, L. In vivo study of nanostructured diopside ($CaMgSi_2O_6$) coating on magnesium alloy as biodegradable orthopedic implants. *Appl Surf Sci.* **2014**, *313*, 60-66.
215. Mahamood, R. M.; Akinlabi, E. T. Types of functionally graded materials and their areas of application. In *Functionally Graded Materials*, Mahamood, R. M.; Akinlabi, E. T., eds.; Springer International Publishing: Cham, 2017; pp 9-21.
216. Shuai, C.; Cheng, Y.; Yang, Y.; Peng, S.; Yang, W.; Qi, F. Laser additive manufacturing of Zn-2Al part for bone repair: Formability, microstructure and properties. *J Alloys Compd.* **2019**, *798*, 606-615.
217. Ilich, J. Z.; Kerstetter, J. E. Nutrition in bone health revisited: a story beyond calcium. *J Am Coll Nutr.* **2000**, *19*, 715-737.
218. Atkins, G. J.; Welldon, K. J.; Halbout, P.; Findlay, D. M. Strontium ranelate treatment of human primary osteoblasts promotes an osteocyte-like phenotype while eliciting an osteoprotegerin response. *Osteoporos Int.* **2009**, *20*, 653-664.
219. Qin, H.; Zhao, Y.; An, Z.; Cheng, M.; Wang, Q.; Cheng, T.; Wang, Q.; Wang, J.; Jiang, Y.; Zhang, X.; Yuan, G. Enhanced antibacterial properties, biocompatibility, and corrosion resistance of degradable Mg-Nd-Zn-Zr alloy. *Biomaterials.* **2015**, *53*, 211-220.
220. Medical Devices Business Services, I. 3.5mm, 4.5mm Locking Compression Plate (LCP®). https://www.jnjmedicaldevices.com/en-US/product/35mm-45mm-locking-compression-plate-lcpr. Accessed May 10, 2021.
221. Buzolin, R. H.; Mohedano, M.; Mendis, C. L.; Mingo, B.; Tolnai, D.; Blawert, C.; Kainer, K. U.; Pinto, H.; Hort, N. As cast microstructures on the mechanical and corrosion behaviour of ZK40 modified with Gd and Nd additions. *Mater Sci Eng A.* **2017**, *682*, 238-247.
222. Zhao, X.; Shi, L. L.; Xu, J. A Comparison of corrosion behavior in saline environment: rare earth metals (Y, Nd, Gd, Dy) for alloying of biodegradable magnesium alloys. *J Mater Sci Technol.* **2013**, *29*, 781-787.
223. Li, Y.; Jahr, H.; Zhang, X. Y.; Leeflang, M. A.; Li, W.; Pouran, B.; Tichelaar, F. D.; Weinans, H.; Zhou, J.; Zadpoor, A. A. Biodegradation-affected fatigue behavior of additively manufactured porous magnesium. *Addit Manuf.* **2019**, *28*, 299-311.
224. Wei, K.; Gao, M.; Wang, Z.; Zeng, X. Effect of energy input on formability, microstructure and mechanical properties of selective laser melted AZ91D magnesium alloy. *Mater Sci Eng A.* **2014**, *611*, 212-222.
225. Zhang, B.; Liao, H.; Coddet, C. Effects of processing parameters on properties of selective laser melting Mg–9%Al powder mixture. *Mater Des.* **2012**, *34*, 753-758.
226. Shuai, C.; Yang, Y.; Wu, P.; Lin, X.; Liu, Y.; Zhou, Y.; Feng, P.; Liu, X.;

Peng, S. Laser rapid solidification improves corrosion behavior of Mg-Zn-Zr alloy. *J Alloys Compd.* **2017**, *691*, 961-969.

227. Wei, K.; Wang, Z.; Zeng, X. Influence of element vaporization on formability, composition, microstructure, and mechanical performance of the selective laser melted Mg–Zn–Zr components. *Mater Lett.* **2015**, *156*, 187-190.
228. Salehi, M.; Maleksaeedi, S.; Sapari, M. A. B.; Nai, M. L. S.; Meenashisundaram, G. K.; Gupta, M. Additive manufacturing of magnesium–zinc–zirconium (ZK) alloys via capillary-mediated binderless three-dimensional printing. *Mater Des.* **2019**, *169*, 107683.
229. He, C.; Bin, S.; Wu, P.; Gao, C.; Feng, P.; Yang, Y.; Liu, L.; Zhou, Y.; Zhao, M.; Yang, S.; Shuai, C. Microstructure evolution and biodegradation behavior of laser rapid solidified Mg–Al–Zn alloy. *Metals (Basel).* **2017**, *7*, 105.
230. Shuai, C.; He, C.; Feng, P.; Guo, W.; Gao, C.; Wu, P.; Yang, Y.; Bin, S. Biodegradation mechanisms of selective laser-melted Mg–xAl–Zn alloy: grain size and intermetallic phase. *Virtual Phys Prototyp.* **2018**, *13*, 59-69.

Received: June 1, 2021
Revised: July 14, 2021
Accepted: August 16, 2021
Available online: September 28, 2021